Groundwater quality and its implications for domestic and agricultural water supplies in a semi-arid river basin of Niger

Boukari Issoufou Ousmane[1] · Yahaya Nazoumou[1,2] · Guillaume Favreau[3] · Maman Sani Abdou Babaye[4] · Rabilou Abdou Mahaman[1] · Marie Boucher[1,3] · James P.R. Sorensen[5] · Alan M. MacDonald[6] · Richard Graham Taylor[7]

[1]Département de Géologie, Faculté des Sciences et Techniques, Université Abdou Moumouni, Niamey, Niger

[2]Autorité de gestion des ressources en eaux souterraines du Niger

[3]Univ. Grenoble Alpes, IRD, CNRS, Grenoble INP, IGE, 38000 Grenoble, France

[4]Département de Géologie, Faculté des Sciences et Techniques, UMR SERMUG, Université Dan Dicko Dankoulodo, Maradi, Niger

[5]British Geological Survey, Maclean Building, Wallingford, OX10 8BB, United Kingdom of Great Britain and Northern Ireland UK

[6]British Geological Survey, Lyell Centre, Research Avenue South, Edinburgh EH14 4AP, United Kingdom of Great Britain and Northern Ireland UK

[7]Department of Geography, University College London, London WC1E 6BT, United Kingdom of Great Britain and Northern Ireland UK

Abstract

In the River Goulbi Maradi Basin (RGMB), groundwater is a vital source of drinking water and plays a central role in the region's socio-economic development. The quality and suitability of groundwater for irrigation and drinking-water remain inadequately understood. We examine hydrochemical analyses of 35 groundwater samples from the shallow alluvial (17) and underlying Continental Hamadien (CH) sandstone (18) aquifers and evaluate these against standard measures of their suitability for drinking water (World Health Organization (WHO) guideline values) and irrigation (i.e. sodium adsorption ratio, sodium percentage, and the residual sodium carbonate). Hydrochemical facies are principally of Na-HCO_3 and Na-Cl types. Bivariate plots combined with saturation indices and electrical conductivity monitoring indicate that the main hydrogeochemical processes influencing groundwater quality are cation exchange in the CH aquifer and solute leaching from soils during focused recharge in the alluvial aquifer. 76% (13/17) of groundwater samples from the alluvial aquifer were suitable for irrigation compared to 38% (6/16) of the

samples from the CH. The identification of high fluoride concentrations exceeding the WHO drinking-water guideline value (> 1.5 mg/L) in 33% (6/18) of samples from the CH aquifer and 18% (3/17) in the alluvial aquifer, and their respective attribution to the release of fluoride of geogenic origin through cation exchange and local use of fluorapatite fertilisers, provide valuable insight into efforts to address the on-going challenge of fluorosis in the Maradi region of Niger and more widely across African drylands. The health consequences of the widespread observation of Mn in concentrations exceeding the new WHO guideline value (0.08 mg/L) in the alluvial aquifer (6/9 samples), often alongside elevated Fe concentrations, are unclear.

Keywords hydrochemistry · groundwater · water-rock interactions · Sahelian zone

Introduction

Groundwater is a vital source of fresh water in many parts of tropical Africa (MacDonald et al. 2012; Gaye & Tindimugaya 2019). From rural areas to big cities, there remains considerable dependence on groundwater either solely or in conjunction with surface water to meet water needs for drinking, livestock rearing, industry, and irrigation (Nazoumou et al. 2016; Cobbing and Hiller 2019). Due to the rapid growth of population and urbanization (UN 2019), and in pursuit of the United Nations (UN) Sustainable Development Goals (SDGs), groundwater withdrawals are expected to increase substantially (Gaye and Tindimugaya 2019; Cobbing 2020) to address rapid increases in demand for domestic water supplies, SDG 6 (water for all) (Adams et al. 2018) and irrigation for food security, SDG 2 (zero hunger) (Altchenko and Villholth 2015; Nazoumou et al. 2016). Additionally, due to their high and underexploited potential in some regions and their resilience to climate variability and change (Cuthbert et al. 2019; Taylor et al. 2022), groundwater discharges play a fundamental role in maintaining and restoring ecosystems (Carter & Parker 2009; Taylor et al. 2013; Abdou Mahaman et al. 2022).

In the central Sahel, rainfall is highly variable in time and space (Lebel and Ali 2009). As a result, surface water resources are often ephemeral and insufficient to sustain sharply rising freshwater demand of increasing populations and socio-economic development (Mahe et al. 2005; Descroix et al. 2009). Here, groundwater is consistently the only perennial source of freshwater (Favreau et al. 2009, 2012; Abdou Babaye et al. 2019) to support poverty alleviation (Favreau et al. 2009, 2012; Nazoumou et al. 2016) and adaptation to climate variability and change; the latter

is associated with increased intensity and severity of droughts and floods (Tschakert et al. 2010; Taylor et al. 2013; Elagib et al. 2021). Despite this fundamental role of groundwater in supporting climate-resilient, socio-economic development, and ecosystem function, data on groundwater systems are often sparse and the current state of knowledge of groundwater systems in the Sahel is limited (MacDonald et al. 2012; Xu et al. 2019).

In the Sahel, substantial groundwater volumes are considered to be stored in regional sedimentary aquifers (Favreau et al. 2012) and several recent studies have sought to resolve the processes that govern groundwater recharge (Favreau et al. 2009; Abdou Babaye et al. 2019; Cuthbert et al. 2019; Goni et al. 2021). An increase in surface runoff has been observed in response to the modification of soil properties and infiltration capacities caused by clearing perennial vegetation (Leblanc et al. 2008; Mahe et al. 2013). This land-cover change has led to sharp increases in surface runoff amplifying river flow and the size and number of ephemeral ponds in central Sahel (Descroix et al. 2009, 2012). Widespread connectivity of surface water to aquifers is vital to groundwater replenishment, even during drought years (Favreau et al. 2009). Notwithstanding the knowledge about quantity and renewal of groundwater that play an indispensable role in the drylands of the Sahel, there is a paucity of data on their suitability for different uses and the hydrogeochemical processes controlling these.

Groundwater is often perceived as a safe and reliable source of water for drinking. Less attention is paid to groundwater quality analyses. As a consequence, the understanding of hydrogeochemical processes and the ability to manage and protect groundwater sources are restricted (Lapworth et al. 2022). To focus greater attention towards groundwater quality is needed. Groundwater in unconfined aquifers is more vulnerable to natural and anthropogenic contamination (Favreau et al. 2009; Lapworth et al. 2012, 2017; Onipe et al. 2020). Due to significant pressures from anthropogenic activities and climate variability, the protection of groundwater resources is necessary to sustain human health, groundwater-dependent livelihoods, and ecosystems (Lapworth et al. 2022). Some land-use change and inadequate management of anthropogenic waste contribute to chemical and organic contamination of groundwater (Ibrahim et al. 2014; Boubacar Hassane et al. 2015). This poses health risks to hundreds of millions of people (WHO 2019) and livestock raising. In addition, there is a direct connection between stores containing groundwater and their status and utility in terms of quality (Gleeson et al. 2020). Natural

processes associated with local geology can affect groundwater quality, through rock-water interactions such as ion exchange and weathering (Abdou Babaye et al. 2019; Zhao et al. 2021).

In the River Goulbi Maradi Basin (RGMB), surface waters are limited in time and space so that the basin's water supply and irrigation derive exclusively from groundwater within a shallow Quaternary alluvial aquifer, largely constrained to the river's floodplain, and an underlying regional Upper Cretaceous sandstone aquifer known as the Continental Hamadien (CH). Recently, a multi-village water supply development program has been planned to increase access to drinking-water in the framework of the National Water, Hygiene and Sanitation Program of Niger (PROSEHA) (MHA 2016); intensive pumping is proposed from deep boreholes, screened in the lower part of the CH aquifer that is thought to be replenished via leakage from the overlying alluvial aquifer (Issoufou Ousmane et al. 2023).

Few water quality assessments have been conducted in the RGMB and the Sahel more broadly. High concentrations of fluoride have, however, been recorded in groundwater pumped from deep boreholes in the RGMB and associated with cases of skeletal and dental fluorosis (FIDH 2002; Laatar et al. 2003). The Ministry of Hydraulics and Sanitation has since ordered the closure of many dug wells and boreholes due to high fluoride concentrations (MHA 2020). Given the continuing uncertainty regarding the quality of groundwater in the RGMB and growing dependence upon groundwater to provide a climate-resilient source of water for domestic and agricultural purposes, the objectives of this study are: (1) to examine the hydrochemical characteristics of groundwater within shallow alluvial and underlying Continental Hamadien aquifers, and (2) to determine the processes governing groundwater mineralization, including the occurrence of locally high fluoride concentrations. The results of this study are intended to inform the planning and management of groundwater in advancing progress towards the UN SDGs in Niger.

Study area

The RGMB is located in southeastern Niger of the south-central Sahel and lies within the southeastern edge of the Iullemmeden sedimentary basin (Fig. 1a and b) between latitudes 13°00' and 13°48' North and between longitudes 6°35' and 7°30' East. It constitutes the Nigerien part of the transboundary RGMB shared between the Maradi Region and northern Nigeria (Fig.1c) and is

bounded to the north by the Goulbi Kabba fossil valley and, to the west by the Goulbi Bounsourou valley. This region is one of the most densely populated in Niger with between 81 and 105 inhabitants/km^2 (INS 2012, 2018). The River Goulbi Maradi is the only source of surface water; the river is seasonal, flowing episodically, from July to October depending on local rainfall and as a result of releases from the Jibya dam in Nigeria (storage capacity: 142 million m^3).

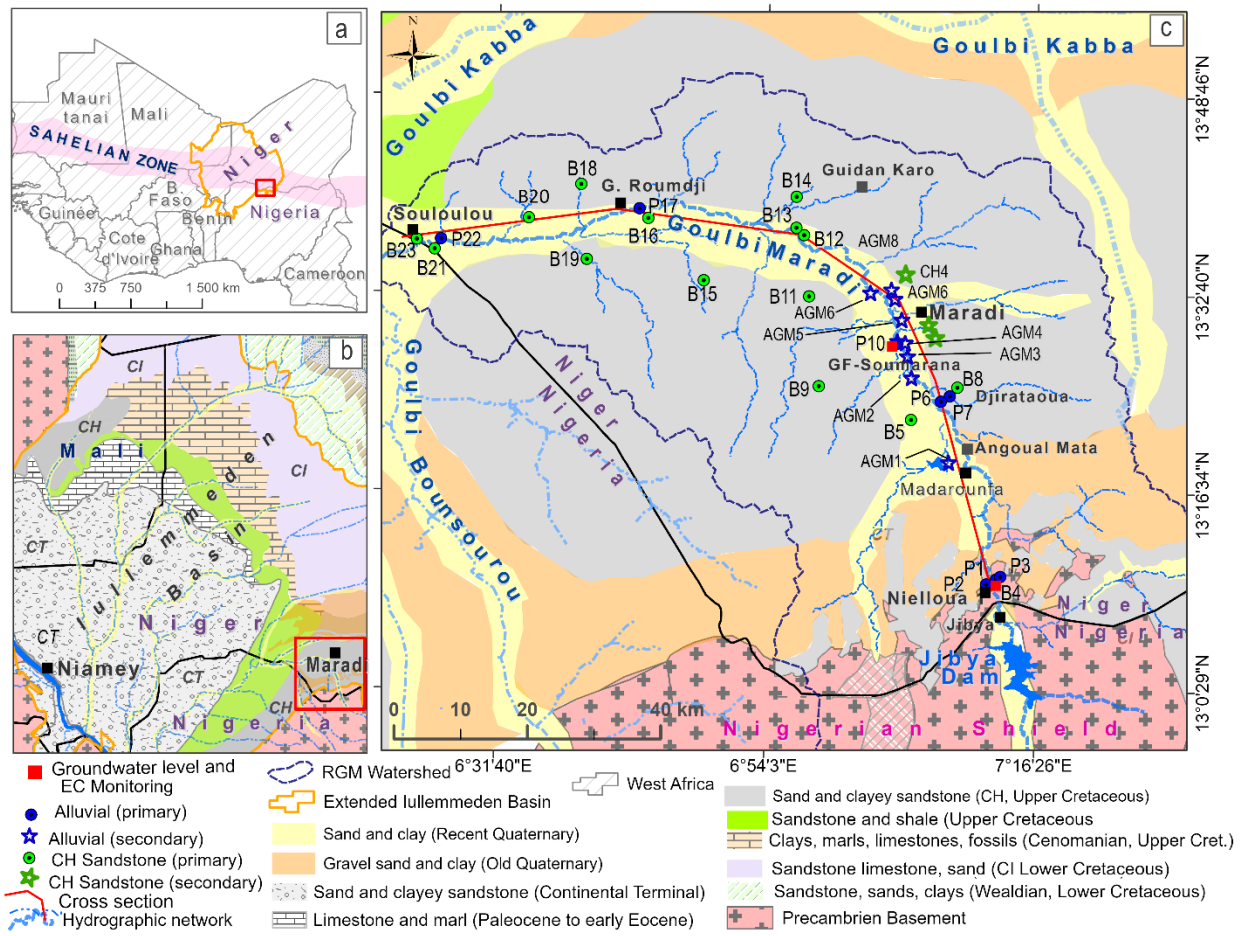

Fig. 1 Maps of the study area: **a** West Africa showing its context in the location of the Sahelian zone; **b** the surface geology and regional drainage of the Iullemmeden basin; **c** the surface geology and drainage of the River Goulbi Maradi Basin (RGMB)

The climate is semi-arid, featuring a single rainy season (June to early October) that is controlled by the African Monsoon (hot and humid), and a long dry season that occurs from November to May and is governed by the Harmattan (dry and very hot wind) coming from the Sahara desert (Issa Lélé & Lamb 2010). Data from the Maradi Airport meteorological station

indicate that the mean annual rainfall is 520 mm (1960-2021); mean monthly air temperatures range between 25 and 35°C; and mean monthly potential evapotranspiration varies between 150 and 210 mm (1984-2010).

The geological context consists of Quaternary formations, the Continental Hamadien (CH) of the Upper Cretaceous, and the crystalline to crystallophyllian Precambrian basement. The Quaternary is characterized by alluvium encountered in the valley with a thickness of up to 30 m, and aeolian deposits formed on the plateaux comprising reddish sand with subordinate clay, 5 to 10 m thick at maximum (BRGM 1978; Durand et al. 1981; Issoufou Ousmane et al. 2021). The CH, surmounted by dune sands on the plateaux and alluvium in the valleys, derives from continental deposits, which represent the lateral equivalent of a marine deposit formed in the Upper Cretaceous (Dikouma 1990; Greigert 1966). In the RGMB specifically, analyses of lithological logs of wells and boreholes reveal that CH is composed of pebbly sand series upstream, clays sandstone series downstream, and Farak-type sandstones localized at the base of the ensemble (Issoufou Ousmane et al. 2023) (Fig. 2). The Precambrian basement consists of granites, gneisses, and schists of Paleoproterozoic to Cambrian age and is exposed in the southern part of the study area along the Nigerian border in an east-west direction. It is in geological continuity with the northern Nigerian shield mobile zone (Mignon 1970; Hazell et al. 1992; Baraou Idi 2018).

Hydrogeologically, the alluvial aquifer has a depth that varies from up to 4 m in the RGMB upstream to 18 m downstream. The aquifer extends laterally across the valley by 1.5 to 4 km and is used mainly for irrigation and population water supply. The underlying CH aquifer is regional in scale and encompasses Niger, Nigeria, and Benin (OSS 2008). Issoufou Ousmane et al. (2023) show that the alluvial and CH aquifer are in hydraulic continuity.

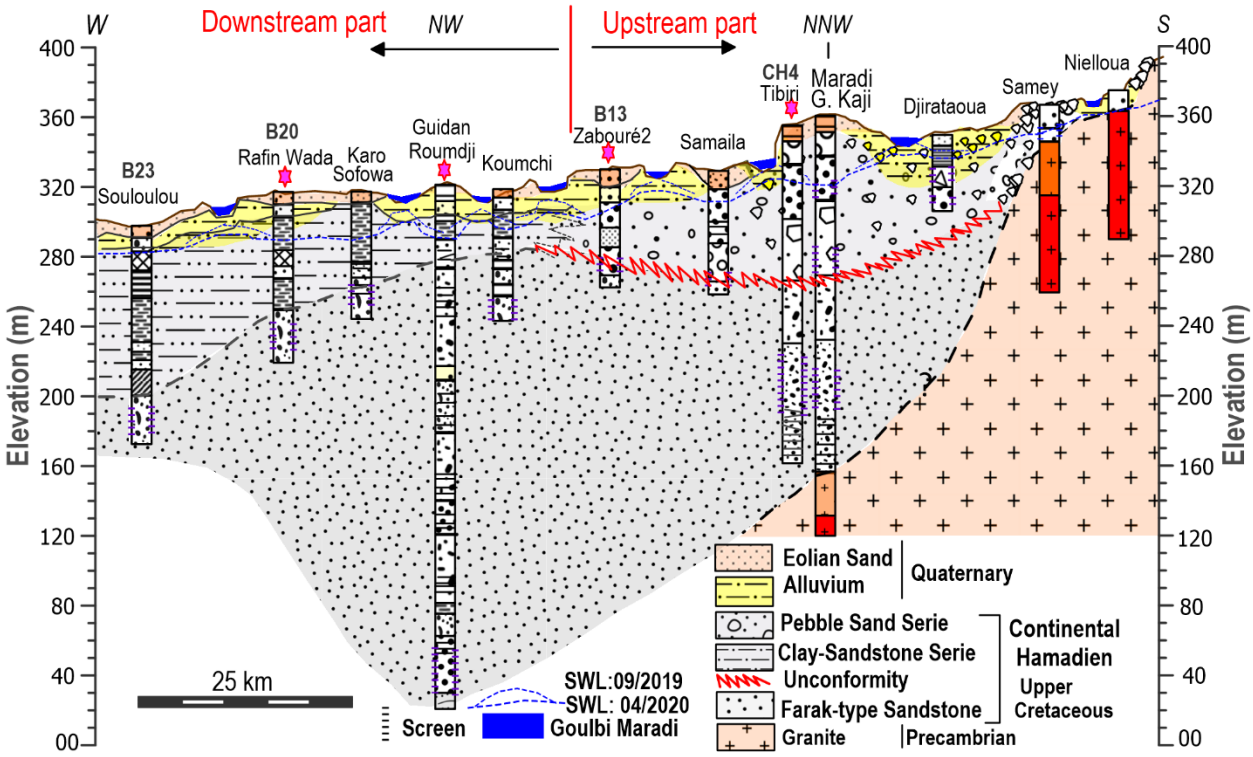

Fig. 2 Upstream-downstream hydrogeological section along the River Goulbi Maradi as shown in Fig. 1c (modify from Issoufou Ousmane et al. 2023). Boreholes with stars are closed because F^{-1} >1.5 mg/L.

Material and methods

Sampling and analytical approaches

In this study, 23 samples comprising 9 observation wells (piezometers) within the Quaternary alluvial aquifer and 14 boreholes used for drinking-water supplies from the CH were collected in November 2018 (Fig. 1c). Boreholes screened in the CH aquifer were selected from an existing database with details of total depth drilled, screen depth, and water-table depth (Table 1). Groundwater from the CH aquifer was deliberately sampled from boreholes (B) whose total depth drilled exceeded 60 m with screen intake depths below 40 m in depth. In the alluvial aquifer, piezometers (P) constructed to depths between 6 and 30 m through this research were sampled (Table 1; Fig. 1a); one sampling site (B4) in the alluvial aquifer is a previously constructed borehole supplying drinking water to the town of Nielloua. Prior to sampling recently constructed piezometers, each was pumped with a submersible WaSP (12V) P5 pump (In-Situ Europe Ltd, UK) to purge three times the volume of the stored water in the borehole. Long-established boreholes

were sampled after "wellhead" physicochemical parameters including electrical conductivity (EC), pH, redox potential (E_h), and dissolved oxygen (DO) had stabilized. Measurements of EC, pH, DO, and E_h were carried out using Seven2GoTM pro meters (Mettler Toledo, Switzerland) and temperature using a HI-93510 thermistor thermometer (Hanna® instruments, USA) installed in a flow-through cell sealed from the atmosphere. Probe calibrations were conducted daily. Samples for major ions (cations and anions) were collected in 30 mL Nalgene bottles. Prior to sampling, bottles were washed three times with deionized water and water from the boreholes before being filtered using a 0.45 µm cellulose nitrate membrane. Samples were stored in a cooler to prevent exposure to excessive temperature variations.

Table 1 Characteristics of wells sampled. P: Piezometer, B: Borehole, na: not available, SWL: static water level measured in piezometer / borehole

Site Code	Date	Lat (N) (°)	Long (E) (°)	SWL (m)	Borehole Depth (m)	Screen Depth (m)
Alluvial aquifer						
P1	13/11/2018	13.15838	7.21516	4.22	13	6.5 - 10.5
P2	12/11/2018	13.15756	7.21214	4.93	12	8.5 - 11
P3	12/11/2018	13.15898	7.21720	5.25	06	na
B4	12/11/2018	13.15763	7.21233	4.96	na	na
P6	07/11/2018	13.39977	7.13799	9.25	15	5.2 - 14
P7	17/11/2018	13.40051	7.14204	11.26	19	9.6 - 12.6
P10	09/11/2018	13.47871	7.08163	5.17	11	na
P17	13/11/2018	13.65916	6.72276	17.76	33	23 - 29
P22	08/11/2018	13.61607	6.44799	12.47	25	18 - 24
Continental Hamadien aquifer						
B5	09/11/2018	13.37566	7.10104	14.43	76	37 - 55
B8	16/11/2018	13.41985	7.16488	44.16	83	49 - 61
B9	08/11/2018	13.42048	6.97296	47.45	88	61 - 82
B11	14/11/2018	13.54182	6.95861	27.94	63	51 - 60
B12	15/11/2018	13.62467	6.95102	14.00	74	49 - 70
B13	15/11/2018	13.63459	6.94024	14.82	62	44 - 47
B14	15/11/2018	13.67661	6.94021	30.91	64	49 - 61
B15	13/11/2018	13.56260	6.81250	51.38	91	76 - 88
B16	14/11/2018	13.64616	6.73495	30.62	70	58 - 67
B18	11/11/2018	13.69146	6.64175	40.60	93	66 - 90
B19	10/11/2018	13.59005	6.65027	26.89	61	44 - 58
B20	10/11/2018	13.64548	6.56951	26.14	95	73 - 93
B21	08/11/2018	13.60222	6.43945	19.62	87	65 - 80

B23	08/11/2018	13.61513	6.41468	23.78	145	105 -135

The analysis of anion concentrations of chloride (Cl^{-1}), sulfates (SO_4^{-2}), fluoride (F^{-1}), nitrate (NO_3^{-1}), and nitrite (NO_2^{-1}) was carried out by ion chromatography using a Dionex system (AS50, Thermo Fisher Scientific, USA) at UKCEH, Wallingford, UK. Concentrations of major cations including calcium (Ca^{+2}), magnesium (Mg^{+2}), sodium (Na^{+1}), potassium (K^{+1}), as well as silica (Si), and trace elements comprising silver (Ag), arsenic (As), barium (Ba), copper (Cu), iron (Fe), manganese (Mn), nickel (Ni), Boron (B), plumb (Pb), rubidium (Rb), strontium (Sr), uranium (U), and zinc (Zn) were measured with Inductively Coupled Plasma Mass Spectrometry (ICP-MS-QQQ Agilent 8900) (Agilent Technologies, USA) at BGS Keyworth, UK. Detection limits for major cations range from 2, 0.003, 0.7 and 0.08 mg/L for Ca^{+2}, Mg^{+2} $Na^{+,1}$ and K^{+1}, respectively. For trace elements, expressed in µg/L, the detection limits for Sr, Mn, and Cu (0.2 µg/L), Fe (0.4), As (0.04), Ni and Ag (0.06), Pb (0.03), Rb (0.3), U (0.009), Zn (0.8), B (93 µg/L) and Ba (0.09 µg/L). The robustness of analytical results was checked by computing the Charge-Balance Error (CBE); computed CBEs of less than ±5% were considered robust.

Hydrochemical plots and indices

Analyses sought to assess the suitability of sampled waters for drinking-water supplies and irrigation and identify geochemical processes controlling groundwater mineralization. Analytical results were compared to World Health Organization standards (WHO 2022). Major cations Ca^{+2}, Mg^{+2}, $Na^{+1} + K^{+1}$) and the anions (HCO_3^{-1}, SO_4^{-2}, Cl^{-1}), were represented on trilinear plots of Piper (1944) to identify hydrochemical facies. Diagrams of Gibbs (1970), plotting the ratios of $Na^{+1}/(Na^{+1} + Ca^{+2})$ and $Cl^{-1}/(Cl^{-1} + HCO_3^{-1})$ versus TDS, were implemented to explore natural processes governing the evolution of groundwater hydrochemistry (Li et al. 2016; Su et al. 2019). To identify ion sources, bivariate diagrams and chloro-alkaline indices 1 and 2 (CAI-1 and CAI-2) defined by equations 1 and 2 (ion concentrations in meq/L) as proposed by Schoeller (1965) were employed.

$$CAI - 1 = \frac{Cl^- - (Na^+ + K^+)}{Cl^-} \quad (1)$$

$$CAI - 2 = \frac{Cl^- - (Na^+ + K^+)}{HCO_3^- + SO_4^{2-} + CO_3^{2-} + NO_3^-} \quad (2)$$

CAI-1 and CAI-2 were used to explore the operation of cation exchange between groundwater and the host rock. Scatter plots of major-ion concentrations of [($Na^+ + K^+$) - Cl^-] versus [($Ca^{2+} + Mg^{2+}$) - ($HCO_3^- + SO_4^{2-}$)] proposed by Fisher and Mullican (1997) were also used to trace geochemical processes including cation exchange (Li et al. 2019; Su et al. 2019). To examine potential dissolution and precipitation processes, saturation indices (SI) of key minerals (e.g. halite, gypsum, calcite, dolomite, fluorite) were computed using the speciation model, PHREEQC (Parkhurst and Appelo 2013).

The chemical composition of irrigation water affects both agricultural yield and soil properties. To assess the quality of water for irrigation, the following indicators were employed: sodium adsorption rate (SAR), the percentage of soluble sodium (%Na), and residual sodium carbonate (RSC). The %Na and SAR are valuable parameters in the evaluation process of groundwater suitability for irrigation because they provide a basis for determining sodium alkalinity hazard in irrigation water as they directly relate to the absorption of sodium on the soil surface (Davraz and Özdemir 2014; Li et al. 2016; Zaman et al. 2018). Water characterized by a high %Na and SAR can produce an accumulation of sodium in the soil, which, in turn, can lead to a decrease in macroporosity and the rate of water infiltration. The suitability of irrigation water was also determined by the Wilcox diagram quality (Wilcox 1948) based on the relationship between percent sodium (%Na) and electrical conductivity (EC). According to this classification, irrigated water is classified into four categories: good to permissible, permissible to doubtful, doubtful to unsuitable, and unsuitable. The RSC indicates the deleterious effect of carbonate (CO_3^{-2}) and bicarbonate (HCO_3^{-1}) on the quality of water for agricultural use (Eaton 1950). If the RSC < 1.25 meq/L, water is safe for irrigation, and if it exceeds 2.5 meq/L, the water is considered unsuitable (Richards 1954).

$$\mathrm{SAR} = \frac{\mathrm{Na^+}}{\sqrt{\frac{\mathrm{Ca^{2+}+Mg^{2+}}}{2}}} \tag{3}$$

$$\%\,\mathrm{Na} = \frac{\mathrm{Na^+}}{\mathrm{Ca^{2+}+Mg^{2+}+Na^+ + K^+}} \times 100 \tag{4}$$

$$\mathrm{RSC} = (\mathrm{CO_3^{2-}} + \mathrm{HCO_3^-}) - (\mathrm{Ca^{2+}} + \mathrm{Mg^{2+}}) \tag{5}$$

These parameters are expressed by equations 3 to 5 in which the cations and anions are in concentrations expressed in meq/L.

Groundwater and surface water monitoring

To better understand the relationship between surface water and groundwater, as well as their seasonal dynamics, high frequency (hourly) monitoring of groundwater levels (GWL) and electrical conductivity (EC), was implemented in 4 piezometers, Nielloua1, P3, Soumarana1, and GF-Soumarana, all screened in the alluvial aquifer. GWL and EC monitoring was undertaken at Nielloua1 and Soumarana1 by the Maradi Regional Direction of Hydraulics and Sanitation (DRH/A-Maradi, Ministry of Hydraulics and Sanitation) from May 2015 (Nielloua1) and September 2016 (Soumarana1) to December 2020, using CTD-Diver dataloggers (Van Essen Instruments). At P3 and GF-Soumarana, GWL and EC were monitored using dataloggers Aqua TROLL 200 and Level TROLL 500 (In-Situ Inc.) from June 2017 to April 2020. The river's stage height was measured manually at Nielloua, through readings on a stream-gauging station, twice a day, in the morning and the evening. Topographic surveys were conducted to enable a comparison between river stage and groundwater levels in the underlying alluvium.

Secondary data

Secondary datasets were also consulted in this study to supplement primary data. Secondary data, consisting of 12 physico-chemical analyses of water samples, were provided by DRH/A-Maradi (Direction Régionale de l'Hydraulique de l'Assainissement). Among these, 8 water samples were collected from piezometers screened in the shallow alluvial aquifer in May 2022, 3 water samples from the CH aquifer were collected from boreholes of drinking-water supply in October 2018, and 1 water sample from CH aquifer collected in April 2000 (Table S1). Analysis of all these samples was performed at the DRH/A-Maradi water quality laboratory. The physico-chemical elements measured in the field and analyzed in the laboratory included respectively the water temperature, EC, and pH, as well as Na^{+1}, Ca^{+2}, Mg^{+2}, K^{+1}, Fe^{+2}, HCO_3^{-1}, Cl^{-1}, SO_4^{-2}, NO_3^{-1}, NO_2^{-1}, and, F^{-1}. Information on sampled boreholes includes total depth drilled, screen depth and water-table depth. All data were considered in the interpretation of hydrogeochemical processes affecting groundwater mineralization.

Results

Hydrochemistry of sampled groundwater

Physicochemical characteristics of groundwater sampled in the alluvial and CH aquifers are provided in Table 2. This table includes computations of basic statistics including the maximum (Max), minimum (Min), average, median, and standard deviation (SD). Sampled groundwater is primarily acidic with pH values ranging between 5.5 and 6.9 in the alluvium and 5.3 and 7.3 pH in the CH with one exception, a value of 8.9 for borehole B23. Moreover, for both aquifers, pH values up to 8.2 were observed in the secondary dataset (Table S1). Groundwater temperatures vary from 29.6 to 31.1°C (median: 30.2°C) in the alluvial aquifer and 30.7 to 33.8°C (median: 31.8°C) in the CH. Electrical conductivity (EC), proxy for total dissolved solids (R^2 = 0.99), in sampled groundwater varies considerably from 78 to 556 µS/cm (mean = 271 µS/cm) in the alluvial aquifer and 67 to 2030 µS/cm (507 µS/cm) in the CH; median values of EC in the alluvial (227 µS/cm) and CH (233 µS/cm) are very similar. In the alluvial aquifer, relatively higher EC values in the alluvium (200 to 550 µS/cm) up to 1300 µS/cm (Table S1) were observed where the piezometers are located in the irrigated land. In the underlying CH aquifer, higher EC values (800 to 2000 µS/cm) were measured in boreholes located in the downstream in the RGMB, where the sampling depths exceeded 60 m. DO range from 0.1 to 2.7 mg/L in the alluvial aquifer and from 0.1 to 4.6 mg/L in the CH aquifer.

Table 2 Physico-chemical parameters of groundwater samples in alluvium and CH aquifers of the River Goulbi Maradi Basin

Alluvial aquifer											
	Samples									Statistical analysis				
	P1	P2	P3	B4	P6	P7	P10	P17	P22	Max	Min	Median	Mean	SD
T (°C)	30.1	29.3	30.4	29.9	30.2	30.3	30.4	31.1	29.6	31.1	29.6	30.2	30.2	0.5
Eh (mV)	139	126	-97	-137	-83	07	69	185	180	185	-137	69	43	125
pH (-)	**6.3**	**6.2**	6.9	7.0	6.6	**6.3**	**6.2**	**5.8**	**5.5**	7.0	5.5	6.3	6.3	0.5
DO (mg/L)	2.7	1.3	0.9	0.3	0.3	0.1	0.1	1.2	0.2	2.7	0.1	0.3	0.8	0.8
EC (µS/cm)	556	143	526	205	260	259	227	185	78	556	78	227	271	163

Continental Hamadien aquifer																			
	Samples														Statistical analysis				
	B5	B8	B9	B11	B12	B13	B14	B15	B16	B18	B19	B20	B21	B23	Max	Min	Median	Mean	SD
T (°C)	31.7	32.5	31.9	31.6	31.9	31.7	32.1	31.1	32.1	33.8	32.9	31.8	30.7	31.1	33.8	30.7	31.8	31.9	0.8
Eh (mV)	251	212	212	215	14	-111	130	194	190	-171	130	68	62	84	251	-171	130	106	126
pH (-)	**5.5**	**6.3**	**5.8**	**5.3**	7.0	7.0	**6.2**	**6.4**	**5.7**	6.7	**6.1**	7.3	6.6	**8.9**	8.9	5.3	6.4	6.5	0.9
DO (mg/L)	1.3	3.5	4.6	0.6	0.2	0.2	0.9	nm	0.7	0.2	3.1	0.2	0.5	0.1	4.6	0.1	0.6	1.2	1.5
EC (µS/cm)	67	88	79	165	932	**2030**	973	187	102	811	146	880	280	360	2030	67	233	507	561

nm: not measured; values exceeding WHO (2022) standard limits are denoted in bold

Hydrochemical results are summarized in Table 3 and Table S1. Two of the 14 sites sampled in the CH aquifer (B5, B20) did not meet the criteria of having a CBE of less than ±5%; one site (B15) with a CBE of -5.5% has been retained. Groundwater facies, plotted in Fig. 3, show both similarities and differences between the two aquifers. Groundwater sampled from the alluvial aquifer (*N*=9) for this study and (*N*=8) for secondary data comprises Na-HCO_3 (*N*=6 and 3) and Ca-HCO_3 (*N*=3 and 5) types, respectively, consistent with recently replenished (unevolved), shallow groundwater. In the underlying CH sandstone aquifer, hydrochemical facies are primarily Na-HCO_3 / Ca-HCO_3 type but include Na-Cl / Ca-Cl types. The Na-Cl facies occur in groundwater sampled from the downstream part of the RGMB.

Table 3 Major and minor-ion and trace element compositions of the alluvial and Continental Hamadien aquifer

	Major and minor ions (mg/L)									Trace elements (µg/L)													CBE (%)
	Ca^{+2}	Mg^{+2}	Na^{+1}	K^{+1}	HCO_3^{-1}	SO_4^{-2}	Cl^{-1}	NO_3^{-1}	F^{-1}	Ag	Ba	Cu	Sr	Fe	As	Mn	Ni	Pb	Rb	B	U	Zn	
WHO (2022)	ng	ng	200	12	ng	250	250	50	1.5	ng	1300	2000	ng	300	10	80	70	10	ng	2400	30	ng	
Alluvial aquifer																							
P1	33	6.3	83	2.7	167	17.9	65	**50**	0.4	0.5	256	1.6	305	63	1.5	21	0.5	0.1	1.2	<93	0.9	5	+0.7
P2	12	2.5	9.4	2.5	57	1.5	6.4	6.5	0.3	0.4	148	0.3	124	**325**	1.6	**113**	0.4	0.2	1.2	<93	0.1	5	+1.3
P3	33	6.1	39	**50**	288	3.0	5.4	0.1	**2.2**	0.3	259	0.6	221	**781**	0.8	**101**	0.3	0.1	9.2	<93	20	3	+1.2
B4	22	4.3	10	4.6	116	1.1	3.9	0.1	0.2	0.3	193	0.3	172	**1350**	**10**	**985**	0.4	0.1	1.8	<93	0.2	5	+1.2
P6	8	2.5	40	1.6	137	4.5	2.1	0.1	0.7	0.3	80	0.5	86	**2870**	2.9	**320**	1.5	1.3	1.5	<93	1.0	20	+2.2
P7	16	4.8	36	2.1	149	4.2	2.9	2.8	0.7	0.3	265	0.4	166	183	3.4	**474**	0.5	0.1	5.5	<93	0.8	7	+2.2
P10	13	4.0	24	6.5	104	8.9	7.8	2.0	0.4	0.3	113	1.1	155	**1360**	0.3	**289**	0.9	3.1	3.6	<93	0.4	7	+2.2
P17	11	2.9	7.6	4.3	46	5.3	2.0	21	0.2	0.3	294	0.5	179	22	0.1	8	0.4	0.4	9.8	<93	0.2	5	-0.8
P22	6	1.2	6.5	2.2	31	2.5	5.8	0.4	0.1	0.3	96	0.5	129	35	0.1	24	0.3	0.3	2.6	<93	0.2	16	+0.6
median	*13*	*4*	*24*	*2.7*	*116*	*4*	*5*	*2*	*0.4*	*0.3*	*193*	*0.5*	*166*	*325*	*1.5*	*113*	*0.4*	*0.2*	*2.6*	-	*0.4*	*5*	-
Continental Hamadien aquifer																							
B5*	<2	<0.003	<0.7	<0.08	27.8	0.27	1.11	10.68	0.12	0.3	<0.1	<0.2	<0.2	<0.4	<0.04	<0.2	<0.06	<0.03	<0.3	<93	<0.01	<0.8	-100
B8	7	2.0	1.9	6.4	24	0.7	3.7	14	0.1	0.3	263	3.6	123	55	0.05	**151**	2.1	0.45	21	<93	0.1	55	+1.3
B9	7	1.7	2.5	6.6	42	0.1	0.6	3.0	0.2	0.3	233	0.9	138	1	<0.04	1.2	1.0	0.06	19	<93	<93	13	+0.4
B11	11	3.4	5.8	7.9	23	9.2	25	6.9	0.1	0.4	416	1.3	183	22	<0.04	4.1	3.5	0.17	19	<93	0.5	09	-3.6
B12	04	0.6	190	2.7	167	79	155	2.3	**4.3**	0.3	25	0.5	160	57	0.34	2.6	0.2	0.11	7.0	1383	0.2	2	-2.4
B13	23	3.7	**397**	6.5	255	181	**395**	0.1	**3.5**	0.3	40	0.5	815	**434**	0.53	33	0.6	1.71	21	2221	0.3	4	-0.9
B14	29	8.1	149	8.7	127	68	196	2.4	0.4	0.4	75	0.7	632	10	0.05	0.6	1.1	0.14	29	925	1.4	4	-1.4
B15	18	2.4	12	7.9	103	1.1	3.4	6.6	0.1	0.3	703	22	595	6	0.18	15	0.7	0.61	13	<93	2.1	30	-1.8
B16	6	1.6	7.4	3.9	48	1.5	2.1	5.5	0.1	0.3	222	3.7	169	31	0.08	1.8	0.5	0.63	16	<93	0.3	6	**-5.5**
B18	85	6.9	67	**13**	158	49	166	0.0	0.0	0.4	146	0.3	2220	73	<0.04	**117**	0.5	0.03	21	216	0.2	2	-1.0
B19	7	2.3	19	4.4	65	2.8	7.0	5.2	0.1	0.3	242	1.3	101	10	<0.04	0.2	0.6	0.16	18	<93	0.4	17	+2.9
B20*	04	1.59	2.7	4.3	195	81.51	120.3	1.38	**3.01**	0.3	170	0.7	67.4	5.4	0.06	1.8	0.54	0.08	13.8	<93	0.26	15	-87.5
B21	9	0.8	53	3.5	157	5.2	5.7	2.8	0.5	0.3	145	0.4	365	8	0.43	5.1	0.1	0.05	3.1	142	5.8	10	-0.0
B23	<2	0.1	81	0.6	164	26	13	0.0	1.1	0.3	30	<0.2	73	3	1.84	0.3	<0.06	<0.03	0.6	246	0.01	1	-1.6
median	*9*	*2*	*36*	*6.5*	*115*	*7.2*	*10*	*2.9*	*0.2*	*0.3*	*184*	*0.9*	*176*	*16*	*0.3*	*25*	*0.6*	*0.2*	*18*	*585*	*0.3*	*7.5*	-

CBE: Charge-Balance Error; ng: no drinking-water guideline value (WHO 2022); concentrations exceeding WHO (2022) drinking-water guideline values are denoted in bold; values with < are below the detection limit; For the samples with stars their CBE is not good and they are therefore not used.

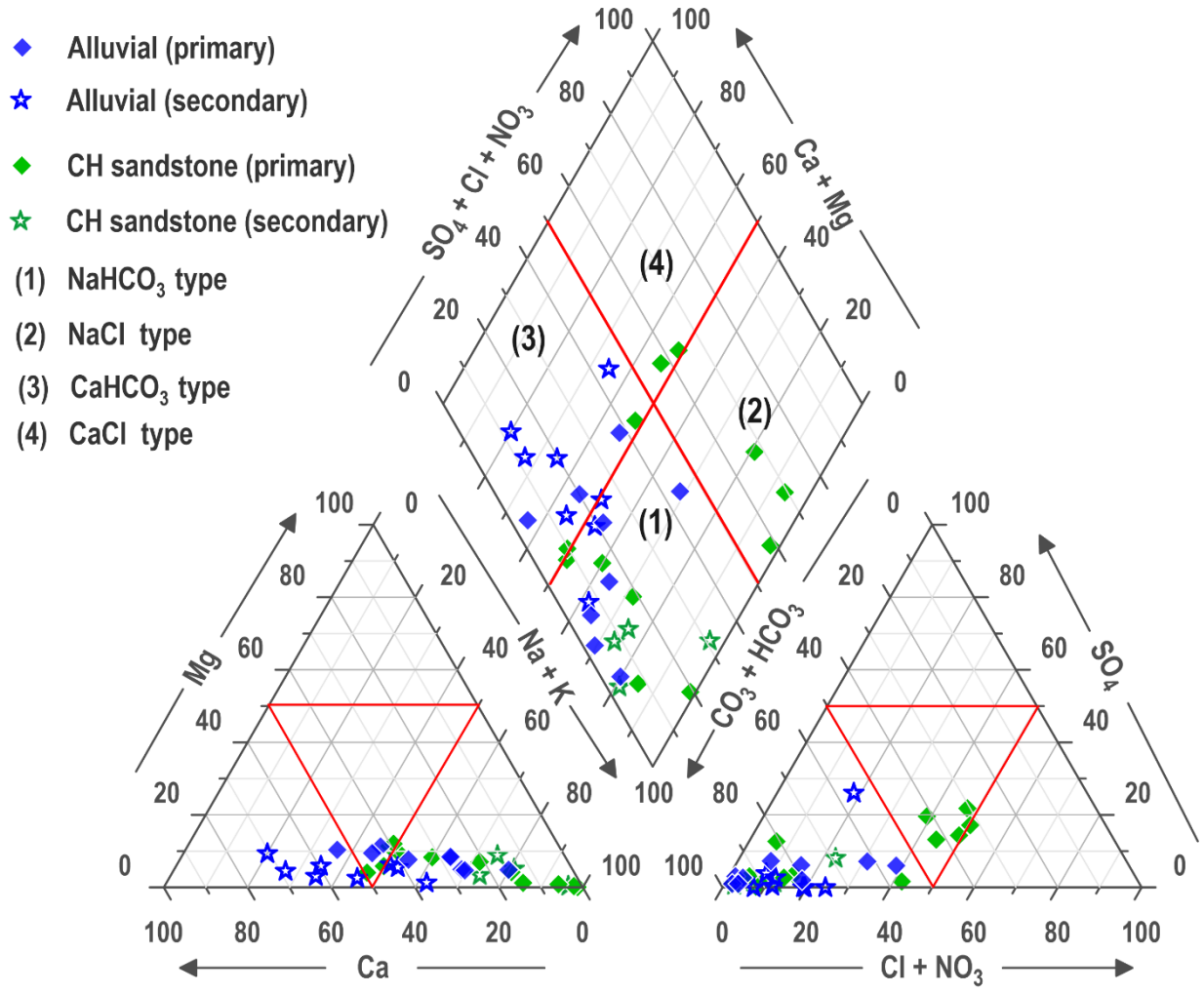

Fig. 3 Piper diagram showing hydrochemical facies of groundwater sampled from the alluvial and Continental Hamadien (CH) aquifers (*N*=34).

Responses in groundwater levels and EC to seasonal rainfall and river flow

Fig. 4 presents hourly hydraulic head and electrical conductivity of the alluvial aquifer, river stage, and daily rainfall at Nielloua (2015-2020) and Soumarana (2017-2020) sites. At Nielloua, the water table resides ~3 m below the riverbed whereas piezometers P3 and Nielloua1 are located at ~50 m and ~270 m from the river channel, respectively. At Soumarana, the water table is ~6 m below the riverbed and piezometers GF-Soumarana and Soumarana1 are located at ~50 m and ~380 m, respectively from the river channel. The hydrographs show pronounced responses to seasonal river flow. Maximum hydraulic heads occur around the end of September around the termination of seasonal river flow and minimum hydraulic heads precede the start of seasonal river flow around

the end of May. At Nielloua, direct comparisons of hydraulic head at P3 and Nielloua1 (Fig. 4a) are limited but indicate (e.g. June to August 2019) higher values of hydraulic head by ~1 m adjacent to the river (P3) relative to observations ~220 m further away from the river. Similarly at Soumarana (Fig. 4b), higher values of hydraulic head are consistently observed adjacent to the river (GF-Soumarana) relative to observations ~330 m further away from the river at Soumarana1. Of note is the sharper, more pronounced rise and fall in hydraulic head at GF-Soumarana, indicative of mounding associated with focused recharge occurring via leakage from seasonal ephemeral river flow; the magnitude of these rises in hydraulic head also relates to the amplitude and duration of seasonal river flow. Higher hydraulic heads observed close to the river at Nielloua and Soumarana clearly reflect the generation of hydraulic gradients driving groundwater flow from focused recharge away from (perpendicular to) the river channel.

Hourly monitoring of the EC of shallow groundwater in the alluvial aquifer shows seasonal variations that coincide roughly with river flow (stage) and a rise in groundwater levels (Fig. 4). At Soumarana, groundwater EC values double from 80 µS/cm in the dry season to 160 µS/cm while the river is flowing. At Nielloua, similarly, groundwater EC varies from 160 µS/cm in the dry season to 200 µS/cm during the monsoon when the river is flowing and groundwater levels rise. In addition, at Nielloua, during dry season, releases from Jibya dam (Fig. 1c) are also shown to lead to focused groundwater recharge (Fig. 4a, area circled in red); this orchestrated recharge event is also associated with an increase in EC of shallow groundwater. The rise in groundwater EC during periods when the river is flowing suggests that focused recharge via riverine infiltration of floodwater discharges is a source of solutes to the alluvial aquifer.

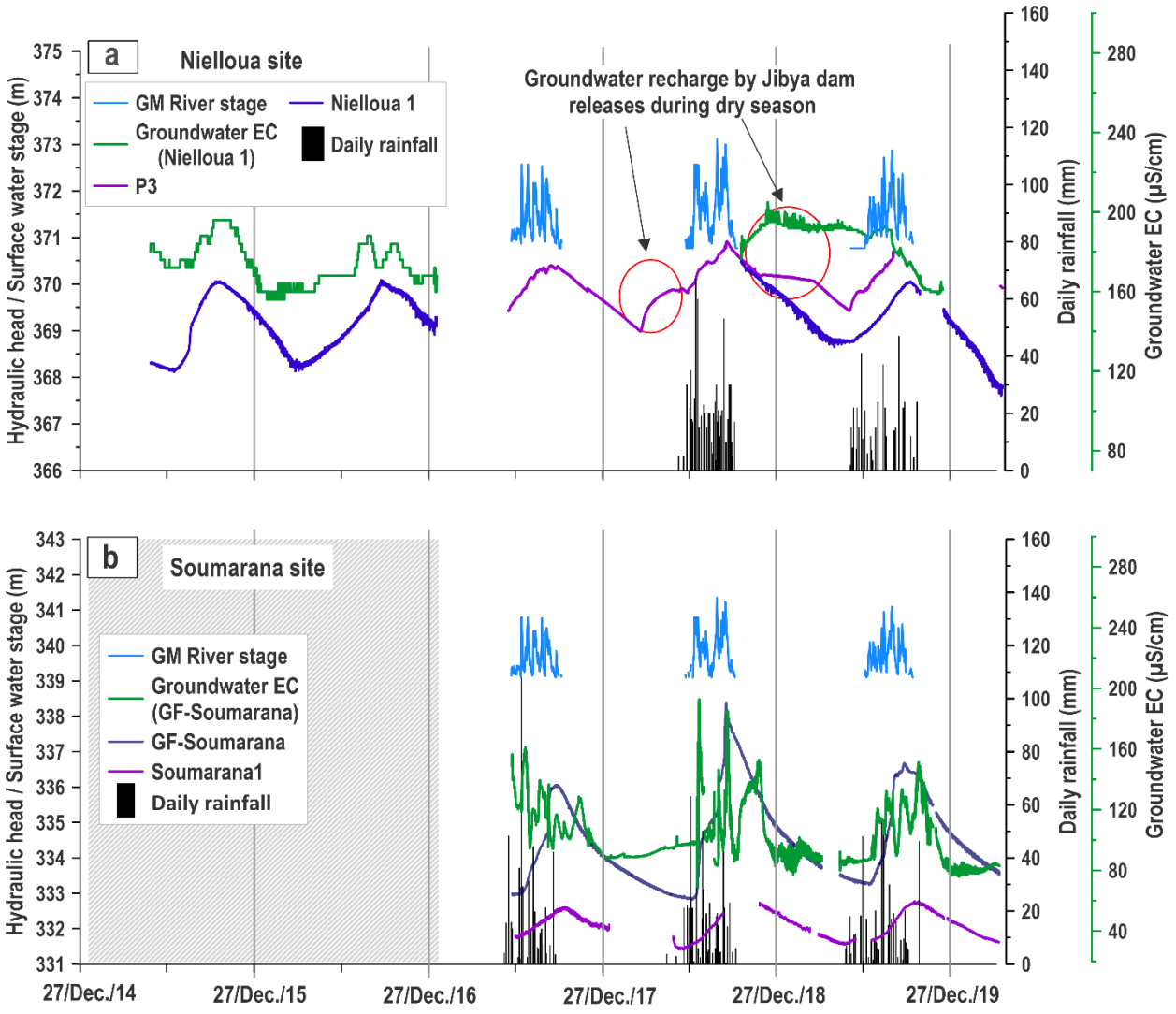

Fig. 4 Seasonal variation in electrical conductivity and hydraulic heads of the alluvial aquifer induced by seasonal river infiltration: **a** Nielloua site, **b** Soumarana site

Controls on groundwater hydrochemistry

To investigate the relationship between the composition of water and natural hydrochemical processes operating at the surface (e.g. recharge sources) and subsurface (e.g. ion exchange, redox reactions, dissolution/precipitation), we employ the relationships between (Na^+, K^+) or (Ca^{2+} and Mg^{2+}) with Cl^-, HCO_3^- or SO_4^{2-} (Subba Rao et al. 2017; Abdou Babaye et al. 2019; Li et al. 2019).

All groundwater samples from the alluvial aquifer plot above the halite dissolution line in Fig. 5a, except one sample from the supplementary data. The bias in ($Na^{+1} + K^{+1}$) over Cl^{-1} suggests halite dissolution is not the primary mechanism responsible for Na^{+1} and Cl^{-1} ions in the alluvial aquifer. For the CH aquifer, the regression (R^2 = 0.88) of ($Na^{+1} + K^{+1}$) vs. Cl^{-1} (plotting above the 1:1 halite dissolution line) with a slope of 1.3 suggests that these ions have a common origin. In drylands, samples deviating from the NaCl dissolution line may be caused by cation exchange and/or silicate dissolution (Su et al. 2019; Huang et al. 2022). Scatter plots relating concentrations of divalent cations (Ca^{+2}, Mg^{+2}) to HCO_3^{-1} (Fig. 5b-c) show that few samples fall along the dissolution line of dolomite ($CaMgCO_3$) or calcite ($CaCO_3$). The relative values of SI (Table 4) are negative and range between -7.3 to -1.3, -10 to -0.91 for dolomite, and -3.5 to -0.4, -4.0 to -0.01 for calcite, respectively, for alluvial and CH aquifer.

In the alluvial aquifer, median concentrations of Ca^{+2} and Mg^{+2} analyzed in this study are 13 and 4 mg/L, respectively. In the supplemental dataset (Table S1), concentrations of Mg^{2+} remain low with a median value of 6 mg/L; higher Ca^{+2} concentrations range from 24 to 280 mg/L with a median value of 71 mg/L (N=8). Statistically significant correlations between HCO_3^- and both Mg^{2+} and Ca^{+2} (R^2 = 0.66 and 0.63, respectively), suggest a common potential mineral source in the alluvial aquifer. In contrast, for the CH samples, both diagrams show an absence of correlation (R^2 = 0.08 and 0.09) between HCO_3^{-1} and Ca^{+2} and Mg^{+2}, inconsistent with a common mineral source (e.g. carbonates) for these ions. Lower median concentrations of Ca^{+2} (9 mg/L) and Mg^{+2} (2 mg/L) may reflect depletion of these ions in the underlying CH aquifer through cation exchange (Rafique et al. 2015; Olaka et al. 2016; Li et al. 2016; Haji et al. 2018; Su et al. 2019).

In the samples from boreholes in the CH aquifer (B12, B13, B14, B18 and B20), high concentrations of Na^{+1} and Cl^{-1}, as well as relatively high concentrations of SO_4^{-2} (50 to 180 mg/L) and F^{-1} (1.1 to 4.3 mg/L) were observed. SO_4^{-2} ions may be associated with gypsum ($CaSO_4{:}2H_2O$) dissolution (Farid et al. 2013; Liu et al. 2020). Similar to the plot for halite (Fig. 5a), Fig. 5d shows that samples from the alluvial aquifer fall above the gypsum line, deviating from a dissolution equilibrium between Ca^{+2} and SO_4^{-2}. Low concentrations of Ca^{2+} (median: 13 mg/L) and SO_4^{-2} (median: 4 mg/L) do not reflect a significant influence of gypsum dissolution on groundwater hydrochemistry in the alluvial aquifer (Farid et al. 2013; Karroum et al. 2017). In the CH aquifer, generally low concentrations of Ca^{2+} (median: 9.0 mg/L) and SO_4^{-2} (7.2 mg/L) plot on either side

of the gypsum dissolution line. Comparatively high concentrations of Ca^{2+} and SO_4^{2-}, ranging respectively from 23 to 85 mg/L and 50 to 180 mg/L, at locations B12, B13, B14, and B18 may reflect gypsum dissolution and the subsequent influence of cation exchange, outlined below.

To explore controls on fluoride concentrations in groundwater in the RGMB, we examine log-log scale correlations between concentrations of F^{-1} and both pH and HCO_3^{-1} (Edmunds and Smedley 2013; Su et al. 2019). The concentration of F^{-1} increases with a rise in concentrations of HCO_3^{-1} and pH (Fig. 5e and f, Table S1), suggesting that higher alkalinity and more alkaline conditions favor the release of F^{-1} into groundwater. These conditions have similarly been observed in the southern main Ethiopian rift by Haji et al. 2018, in the in the western region of the Ordos basin, northwestern China by Su et al. 2019 and in the central Australia, western North America, eastern Brazil and many areas of Africa and Asia by Podgorski & Berg 2022.

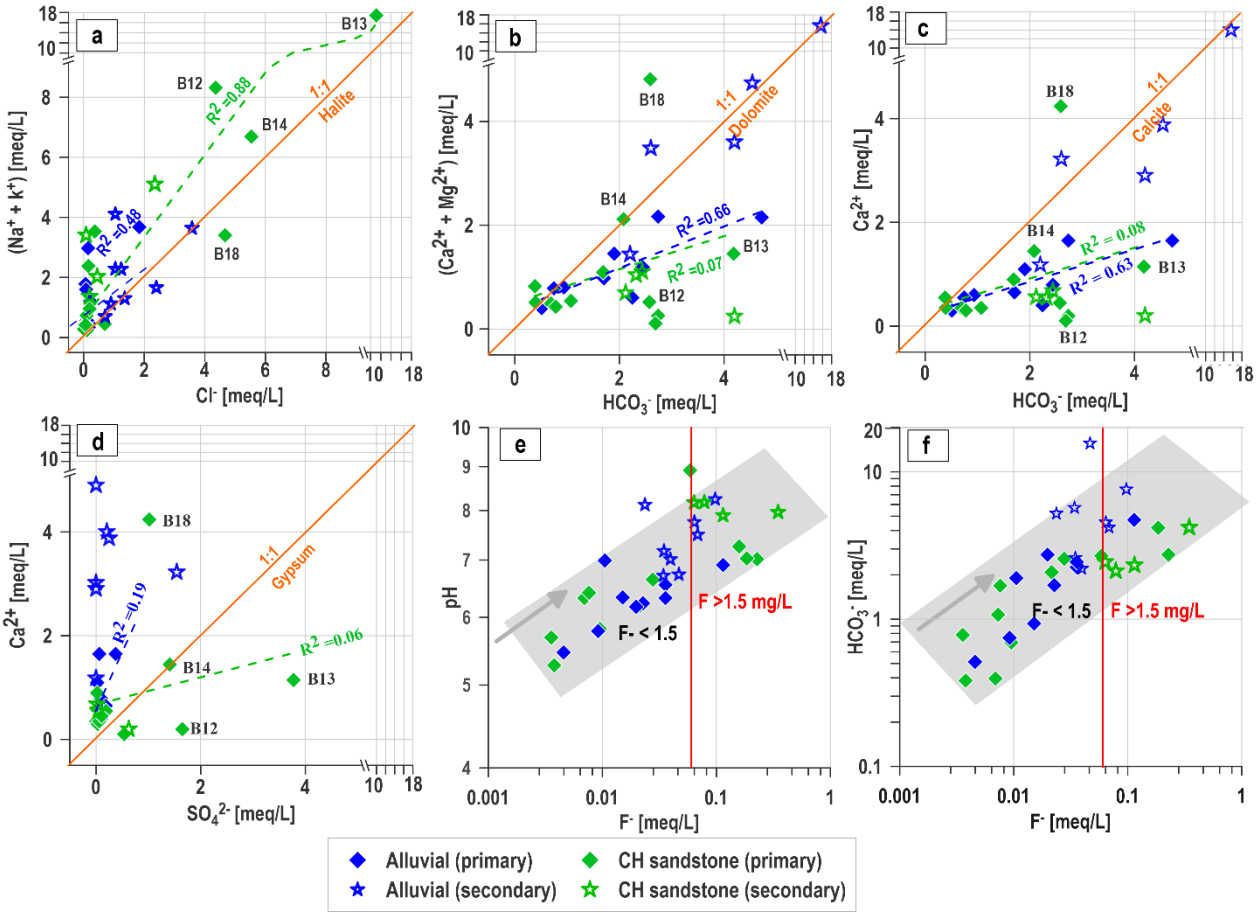

Fig. 5 Scatter plots of the relationships between hydrochemical compositions: **a** (Na^{+1} + K^{+1}) vs. Cl^{-1}, **b** (Ca^{+2} + Mg^{+2}) vs. HCO_3^{-1}, **c** Ca^{+2} vs. HCO_3^{-1}, **d** Ca^{+2} vs. SO_4^{-2}, **e** pH vs. F^{-1}, **f** HCO_3^{-1} vs. F^{-1}

Table 4 Saturation indices (SI) of calcite, dolomite, halite and fluoride Saturation indices (SI) of calcite, dolomite, halite and fluorite

Samples	SI Calcite	SI Dolomite	SI Gypsum	SI Halite	SI Fluorite
Alluvial Aquifer					
P1	-1.47	-3.27	-2.6	-6.85	-2.21
P2	-2.11	-4.49	-3.94	-8.76	-2.76
P3	-0.48	-1.28	-3.37	-8.26	-0.68
P6	-1.72	-3.53	-3.68	-8.62	-2.23
P7	-1.62	-3.36	-3.45	-8.54	-1.95
P10	-1.94	-3.99	-3.18	-8.29	-2.74
P17	-2.78	-5.73	-3.43	-9.37	-3.57
P22	-3.52	-7.34	-3.98	-8.95	-5.04
B4	-0.91	-2.14	-3.86	-8.96	-2.84
Continental Hamadien Aquifer					
B8	-2.67	-5.46	-4.45	-9.69	-3.67
B9	-2.93	-6.05	-5.23	-10.37	-3.41
B11	-3.57	-7.24	-3.2	-8.39	-4.13
B12	-1.56	-3.5	-2.91	-6.13	-2.41
B13	-0.71	-1.81	-1.96	-5.44	-0.62
B14	-1.64	-3.42	-2.15	-6.14	-2.29
B15	-1.6	-3.67	-3.94	-8.94	-3.22
B16	-3.09	-6.34	-4.21	-9.35	
B18	-0.58	-1.81	-1.86	-6.56	-4.35
B19	-2.46	-4.96	-3.89	-8.42	-3.66
B21	-1.52	-3.66	-3.58	-8.08	-2.41
B23	-0.01	-0.91	-3.61	-7.54	-2.49

Evidence presented in the Fig. 5 suggests that mineralization processes in the RGMB are influenced by water-rock interactions that are particularly evident in groundwater samples from the regional CH aquifer. The importance of cation exchange between Na^{+1} adsorbed on clay minerals with Ca^{+2} and Mg^{+2} in groundwater is suggested when values of the chloro-alkaline indices (CAI-1 and CAI-2) are negative (Huang et al. 2022). Furthermore, a significant impact of this exchange on the chemical composition of groundwater is shown when the scatter plot of the diagram [(Na^{+1}

+ K^{+1}) - Cl^{-1}] versus [(Ca^{+2} + Mg^{+2}) - (HCO_3^{-1} + SO_4^{-2})] regresses along the line of slope 1:1 (Li et al. 2019; Su et al. 2019). In the study area, computed values of CAI-1 and CAI-2 (Fig. 6a) are negative in the alluvial and CH aquifer; further, Fig. 6b shows that all the points align along a slope of [(Na^{+1} + K^{+1}) - Cl^{-1}] versus [(Ca^{+2} + Mg^{+2}) - (HCO_3^{-1} + SO_4^{-2})] with correlation coefficients (R^2) of 0.90 and 0.99, respectively for the alluvial and CH aquifers. Evidence from this graphical plot suggests cation exchange is a key hydrochemical process operating in the study area where Na^+ in the aquifer is exchanged for Mg^{+2} and Ca^{+2} ions in the water.

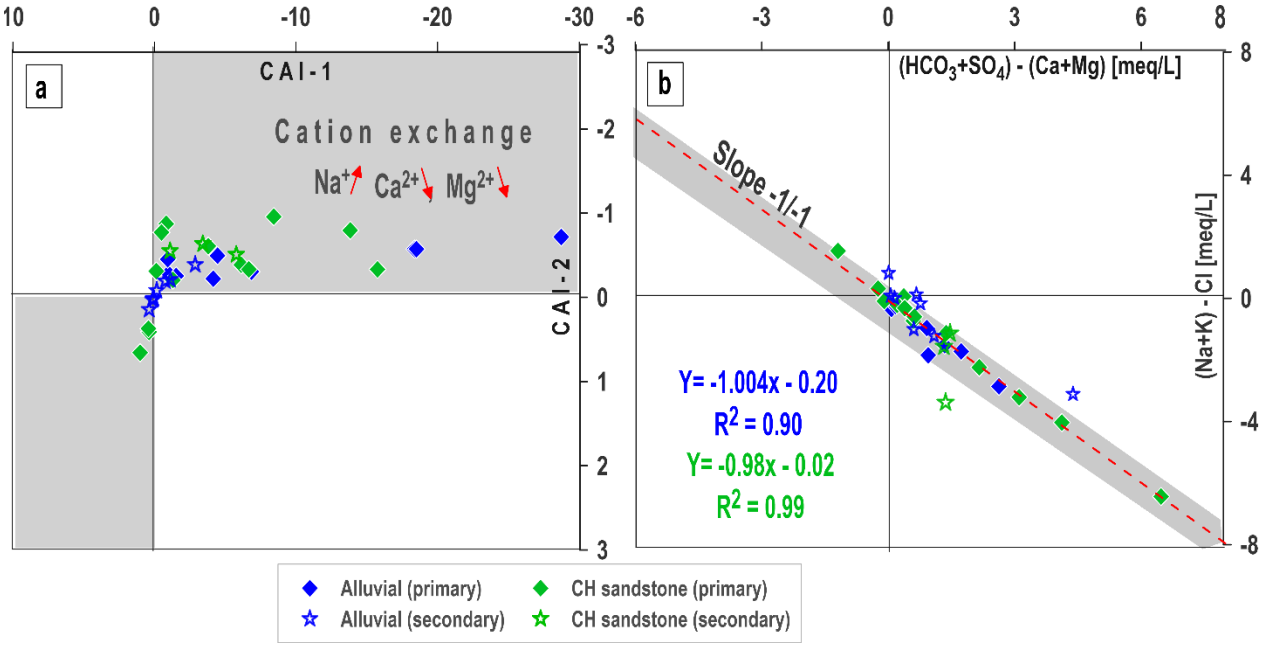

Fig. 6 a Diagram of Chloro-alkaline indices CAI-2 vs. CAI-1 for alluvial and CH aquifer, **b** Diagram (Na^{+1} + K^{+1}) – Cl^{-1} vs. (HCO_3^{-1} + SO_4^{-2}) – (Ca^{+2} + Mg^{+2})

In both aquifers, trace elements Fe and Mn showed high concentrations, particularly in the alluvial aquifer, where values range from 22 to 2870 µg/L with a median of 325 µg/L for Fe and from 8 to 985 µg/L with a median of 113 µg/L for Mn. In the underlying CH aquifer, values range from 1 to 434 µg/L with a median of 16 µg/L for Fe and from 0.2 to 151 µg/L with a median of 25 µg/L for Mn. The high values of Fe and Mn could be controlled by redox reactions, especially in the presence of groundwater with a pH range of 5.5 – 8 and low values of E_h (Rivett et al. 2008; McMahon et al. 2019). In order to highlight the influence of pH and redox conditions on Fe and Mn concentrations, the diagrams E_h (mV) versus pH (-) have been implemented according to each of this element (Fig. 7a, b) (Homoncik et al. 2010). This diagram illustrates that in a pH range

between 6-7 and Eh between -170–70 mV, Fe^{2+} Mn^{2+} have high contractions for the samples from alluvial aquifer, suggesting that Fe and Mn are mobilized trough redox reactions in this aquifer. However, for the CH aquifer, the pH and E_h do not have a significant influence on the Fe and Mn concentrations, thus excluding the influence of redox reactions in the CH aquifer. Moreover, groundwater Fe and Mn simultaneously elevated while Fe concentration being several times to an order of magnitude higher than Mn indicating their co-release process (Fig. 7c, d).

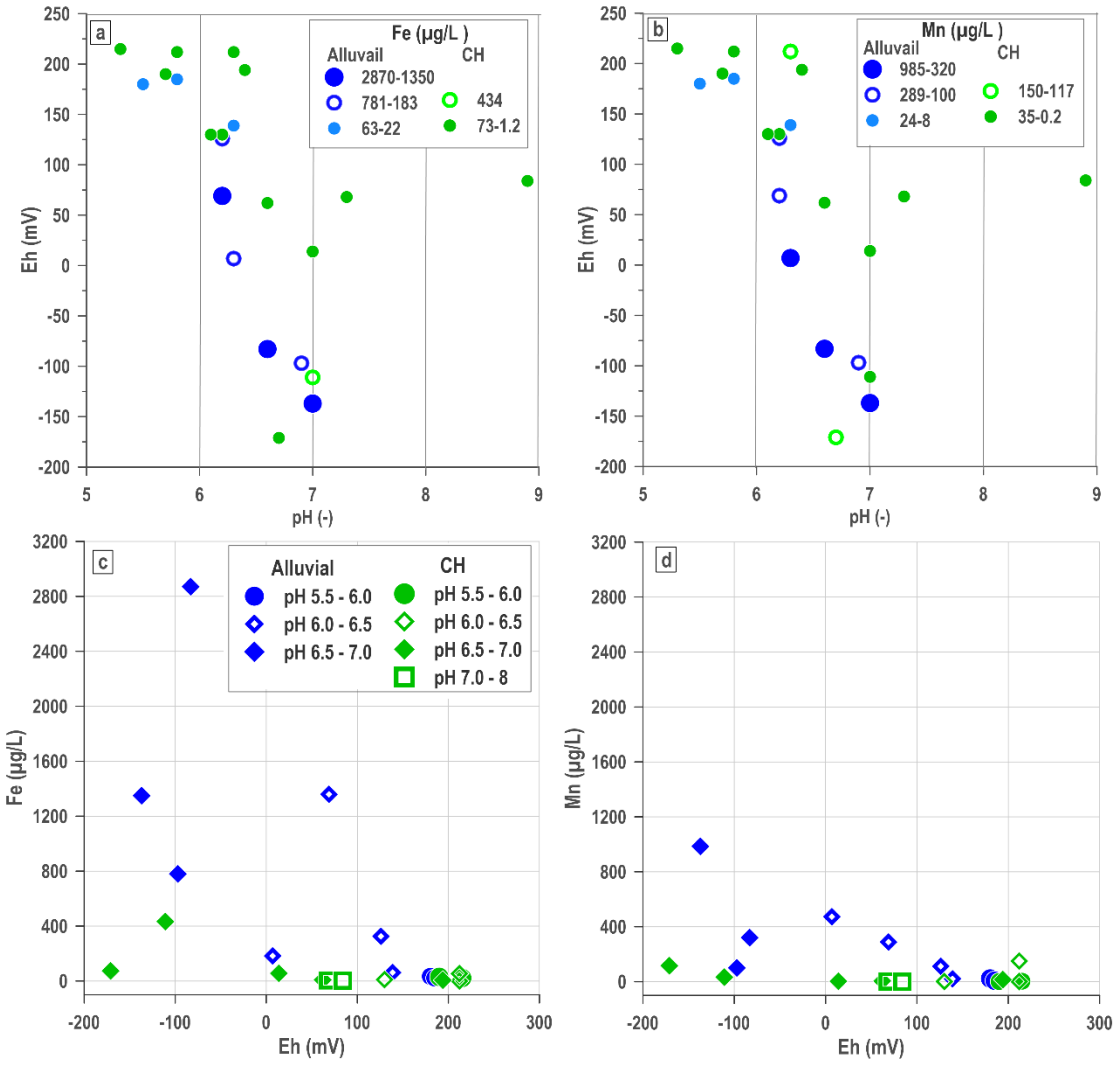

Fig. 7 ab Fe and Mn concentrations as function of Eh vs. pH, **cd** E_h vs. diagram Fe and Mn vs E_h

Quality of groundwater for irrigation

Computed SAR, %Na and RSC values are shown in Table 5 and Table S2. The SAR is ranging between 0.3 and 4.9 meq/L in the alluvial aquifer and from 0.2 to 33 meq/L in the underlying CH

aquifer. The %Na value ranges from 22 to 73 in the alluvial aquifer and 11 to 97 in the CH (Table 5). Calculated values of the RSC range from -0.04 to 2.6 meq/L in the alluvial aquifer, whereas in the CH aquifer, values are more consistent and between -2.2 and 2.9 meq/L (Table 5).

Table 5 Indices defining the suitability of sampled groundwater for irrigation.

	Alluvial aquifer														
	Samples												Statistical analysis		
	P1	P2	P3	B4	P6	P7	P10	P17	P22				Max	Min	Mean
SAR	4.9	0.9	2.3	0.7	4.5	2.8	2.1	0.7	0.3				4.9	0.3	2.1
%Na	62	32	33	22	73	55	47	27	38				73	22	43
RSC	0.56	0.13	2.6	0.45	1.6	1.3	0.72	-0.04	0.11				2.56	-0.04	0.82
	Continental Hamadien aquifer														
	Samples												Statistical analysis		
	B8	B9	B11	B12	B13	B14	B15	B16	B18	B19	B21	B23	Max	Min	Mean
SAR	0.2	0.9	0.5	33	29	8.8	01	0.9	2.6	2.3	6.4	23	32.8	0.2	7.7
%Na	11	14	20	96	91	73	29	38	36	56	79	97	97	11	48
RSC	-0.12	0.20	-0.45	2.5	2.7	-0.05	0.59	0.35	-2.2	0.53	2.1	2.6	2.86	-2.24	0.86

Discussion

Mineralization processes

In tropical drylands, mineralization processes in shallow groundwater are complex as pathways of groundwater recharge and discharge can be multiple. Previous research in endorheic watersheds of southwestern Niger demonstrated that different recharge processes (e.g. focused and diffuse) influence groundwater mineralization (Favreau et al. 2009; Ibrahim et al. 2014). Hassane et al. (2015) observed, for example, that shallow wells (5-15 m) show high and variable EC values (36 to 1617 µS/cm) at the beginning of the rainy season compared to EC values (36−340 µS/cm) in deeper wells (15–30 m). They contend that salts, which accumulate on the soil surface and in the unsaturated zone from high evapotranspiration rates over the dry season, are subsequently leached to groundwater by infiltrating recharge; this process could explain the observed rise in the EC of shallow groundwater at the beginning of the rainy season. Under conditions of focused recharge via infiltration from seasonal ponds (Favreau et al. 2009; Cuthbert et al. 2019), monitoring of shallow groundwater quality reveals an initial rise in the concentrations of major ions (e.g. Mg^{+2}, Ca^{+2}, Na^{+1}, NO_3^{-1}, Cl^{-1}, SO_4^{-2}, HCO_3^{-1}) at the beginning of the rainy season (Elbaz-Poulichet et al. 2002); towards the middle and end of the season, EC reduces and then stabilizes. Furthermore, in

tropical drylands where diffuse recharge occurs, evapotranspiration may result in residual saline pore waters in the unsaturated zone that contribute to the mineralization of groundwater in shallow and deep aquifer systems (Tweed et al. 2011; Foster et al. 2018; Rajmohan et al. 2021).

High-frequency (hourly) monitoring in the shallow alluvial aquifer in the RGBM shows a concomitant seasonal variation in piezometric heads and EC. This seasonal variation is characterized by an increase in piezometric heads and EC during periods when the River GM is flowing. Similarly, releases from the Jibya Dam during the dry season are also associated with an increase in groundwater EC (Fig. 4). This hydraulic and hydrochemical evidence suggests that leakage from the River Goulbi Maradi is a source of focused recharge that increases the EC of groundwater. Also, the absence of a rise in EC during the dry season, especially when there were no water releases from the Jibya dam, suggests that direct evapotranspiration from the shallow aquifer does not play a substantial role in the mineralization process of groundwater. We posit that the observed rise in solute concentrations increasing EC during recharge derive from leaching of solutes from soil surface in and unsaturated zone that contribute to river discharge and focused recharge to groundwater. In addition, the relatively higher Na^{+1} and Ca^{+2} contents in shallow alluvial aquifer could be explained by leaching during the river water infiltration.

Origin of high fluoride groundwater

High fluoride concentrations in groundwater observed in the RGMB have been noted in many parts of the world (Ali et al. 2016; Wang et al. 2020; Nordstrom & Smedley 2022; Podgorski & Berg 2022) and associated with both geological settings and human activity. The geogenic origin of fluoride include the dissolution of fluoride-bearing minerals found in sedimentary, metamorphic, and igneous rocks (Edmunds & Smedley 2013; Olaka et al. 2016; Haji et al. 2018). Human activities that contribute to fluoride contamination of groundwater include the intensification of agriculture that includes use of pesticides and phosphate fertilizers (Kundu & Mandal 2009; Xu et al. 2022).

In drylands, the occurrence of fluoride in groundwater systems is thought primarily to be controlled by cation exchange, rock/soil weathering, and evaporation (Edmunds & Smedley 2013; Su et al. 2019; Wang et al. 2020; Nordstrom & Smedley 2022; Podgorski & Berg 2022). Groundwater sampled from a range of weathered crystalline rock aquifer systems including

metamorphic rocks, intrusive granite, and volcanic rocks have been associated with high fluoride concentrations in Sudan (up to 3.6 mg/L), northeastern Ghana (up to 20 mg/L), and the East African Rift System in Kenya (up to 10.5 mg/L), Uganda (up to 3.0 mg/L), Tanzania (up to 8.8 mg/L), and Ethiopia (up to 12.0 mg/L) (Kut et al. 2016; Olaka et al. 2016; Haji et al. 2018; Ijumulana et al. 2020; Onipe et al. 2020). Weathering and leaching of fluoride-bearing minerals in these rocks, such as biotite, muscovite, fluorite, hornblende, tonalite, mica, and fluorapatite, is a critical process influencing fluoride concentrations in groundwater (Onipe et al. 2020). In the northern Nigeria bordering the study area (Fig. 1c), high fluoride concentrations (0.03 to 10.30 mg/L) were measured in groundwater from weathered crystalline rock aquifer systems including granites, schists, gneisses, and migmatites (Hazell et al. 1992; Dibal et al. 2012; Tukur & Akobundu 2014; Kut et al. 2016; Baraou Idi 2018; Onipe et al. 2020).

In the southeastern and northeastern parts of the Senegal Basin, high concentrations of fluoride in groundwater (1-5.5 mg/L) occur in the deep Maastrichtian aquifer, which consists of clayey sand, lignite intercalation, and sandstone (Travi 1988). In this aquifer, fluoride concentrations generally increase in the direction of groundwater flow. The source of the dissolved fluoride is associated with the occurrence of fluorapatite, particularly in argillaceous deposits. In the sequence of Cretaceous to Quaternary sediments of western Tunisia, high fluoride concentrations were found in groundwater from the Cretaceous 'Complexe Terminal' aquifer (Travi 1988; Edmunds & Smedley 2013). These sediments are also phosphatic, although the relationships between phosphate occurrence and dissolved fluoride concentrations were found to be less clear than in Senegal. High-fluoride groundwaters up to 5 mg/L are also detected in Maiduguri of northeastern Nigeria in boreholes tapping groundwater from the upper and lower zones of the Chad Formation (Dibal et al. 2012); the source of anomalously high fluoride concentrations has yet to be resolved. According to Goni (2006) and Goni et al. (2021), both aquifer horizons are semi-confined to confined and consist of unconsolidated sands separated by clay layers; sediments derive from the alkaline geochemical province of the Jos plateau and contain highly weatherable silicate minerals.

In the RGMB, relatively high fluoride concentrations were measured in the alluvial aquifer (1.8 to 2.2 mg/L) and in the underlying CH aquifer (3.1 to 6.6 mg/L) (Table 3) (Table1 S1). In the alluvial aquifer, most prominently in the secondary data (Table S1) collected close to irrigated

lands, samples with fluoride concentrations above 0.6 mg/L also feature high concentrations of Ca^{+2} (median: 71 mg/L), K^{+1} (median: 29 mg/L), and Cl^{-1} (median: 41 mg/L). Relatively high concentrations of Ca^{+2}, K^{+1}, and F^{-1} in shallow groundwater may indicate anthropogenic sources of these ions from irrigation return flows and the use of chemical fertilizers to increase crop yield (Boubacar Hassane et al. 2015; Lapworth et al. 2017). From field interviews with irrigators and the Regional Direction of Agriculture, fertilizers used in the study area include compost substrates, Di-Ammonium Phosphate (DAP), Nitrogen-Phosphorus-Potassium (NPK), and urea. These fertilizers are very soluble and have a mineral phase, primarily fluorapatite carbonate ($Ca_5(PO_4,CO_3)_3F$) (Mar & Okazaki 2012). The high concentrations of these solutes in association with fluoride in the alluvial aquifer, where water-table depths range from 3 to 10 m in irrigated areas, is consistent with fertilizer as a fluoride source. It was also noted in the alluvial aquifer that concentrations of NO_3^{-1} (0-50 mg/L, median 2.5 and 5 mg/L) (Table 3 and Table S1) are low and may reflect redox conditions enabling denitrification (Rivett et al. 2008). High concentrations of HCO_3^{-1} (130-950 mg/L, median 297 mg/L) and trace elements Fe^{+2} (22 µg/L to 2300 mg/L, median 325 µg/L) and Mn^{2+} (8 to 985 µg/L with a median of 113 µg/L) observed in the shallow alluvial aquifer, are consistent with denitrification (Table 3 and Table S1) (Korom 1992).

For the underlying CH aquifer composed of clayey (Farak-type) sandstone, the depositional environment is continental and the sandstone derives from the erosion and deep weathering of rocks of the Nigerian Shield basement complex (Greigert 1966; Issoufou Ousmane et al. 2023). In these basement rocks, fluoride-bearing minerals such as muscovite, mica and chlorite have been reported (Baraou Idi 2018). Thus, these minerals may be found in the clayey (Farak-type) sandstone and exchange minerals with the groundwater. This argument is supported by the diagram in Fig. 6, showing cation exchange between Na^{+1} adsorbed on clay minerals and Ca^{2+} and Mg^{2+} in groundwater. Higher fluoride concentrations are associated with samples in which Na^{+1} ions are strongly present (Table 3), indicating that cation exchange is a key process in the development of high fluoride concentrations in groundwater. In addition, locally high fluoride concentrations decrease with depth from upstream (120 m) to downstream (80 m). Fig. 8 based on the borehole lithological logs, summarizes observed variations in EC, chemical facies, and fluoride concentrations with depth.

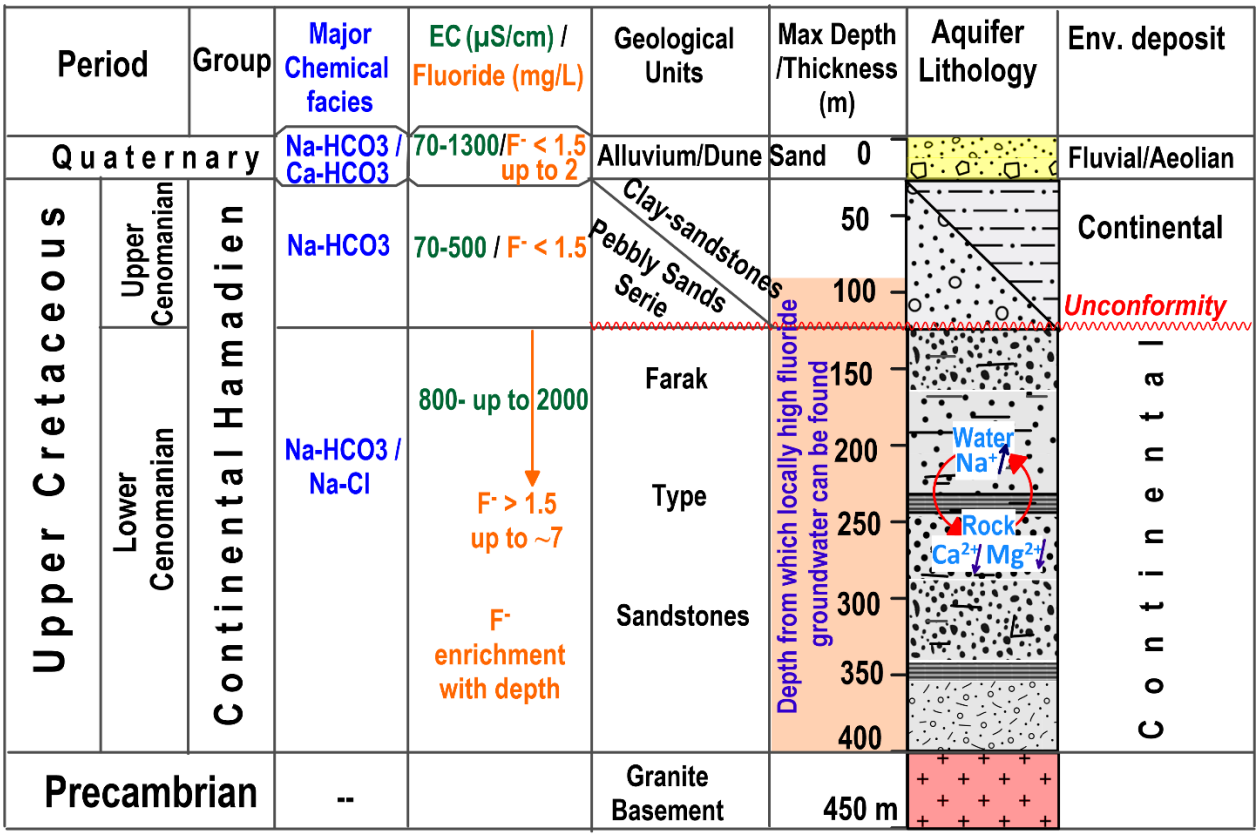

Fig. 8 Lithostratigraphic column of the study area from borehole data analysis showing the variation of electrical conductivity (EC), chemical facies, and fluoride concentration with depth (modified from Issoufou Ousmane et al. 2023).

Groundwater quality for drinking water and irrigation

Solute concentrations in the alluvial and CH aquifers (Fig. 9) were generally below drinking-water guideline values with a few exceptions. Fluoride concentrations (2.2 mg/L) exceeding WHO (2022) guideline values for drinking water based on health concerns (1.5 mg/L) were detected in one sample (P3) in the alluvial aquifer; this sample is located in the upstream part of the RGMB around the Niger-Nigerian border (Fig. 1c) where the alluvium is thin and in contact with weathered granite (Fig. 2). In the CH aquifer, fluoride concentrations exceeding the guideline value were measured in boreholes located downstream (Fig. 1c) at B12 (4.3 mg/L), B13 (3.5 mg/L) and B20 (3.0 mg/L) with well depths of 90 and 62 m, respectively. In these boreholes, the waters have low Ca^{+2} and Mg^{+2} and are hydrochemically of the Na^{+1} / HCO_3^{-1} type and high SO_4^{-2} and Cl^{-1}. In the alluvial

aquifer, concentrations of nitrate at P1 (50 mg/L) and arsenic at B4 (10 µg/L) that are on the borderline of guideline values for health reasons were also observed.

Solute concentrations exceeding WHO (2022) drinking-water guidelines for aesthetic reasons were also observed in both alluvial and CH aquifers (Fig. 9). Although measured physiochemical parameters (Table 2) (EC, pH, DO, T, and E_h) in sampled groundwater meet WHO (2022) guidelines, the salinity of 1 borehole (B13) in the CH with an EC of 2030 µS/cm was excessive, featuring high concentrations of sodium (397 mg/L), chloride (395 mg/L) and iron (434 µg/L).

Concentrations of iron exceeding the guideline value of 300 µg/L and ranging from 325 to 2870 µg/L were also observed at several locations in the alluvial aquifer including P2, P3, B4 P6, and P10 (Fig. 1c). Additionally, concentrations of manganese exceeding value of the WHO (2022) guideline value of 80 µg/L were recorded in the alluvial aquifer at P2, P3, B4, P6, P7 and P10 and in the CH aquifer at B8 and B18 (Fig. 1c). These high concentrations of Fe and Mn observed in the RGMB groundwater, especially in alluvial aquifer, has also been reported in many parts of Africa (Ethiopia, Malawi and Uganda) and are frequently concomitant or associated with high As or NO_3 (Lapworth et al. 2020). In the alluvial aquifer, high concentrations of these two elements appear to be associated with groundwater redox reactions under anoxic conditions at a pH range of 6 and 7, consistent to other studies globally (Homoncik et al. 2010; McMahon et al. 2019). Manganese concentrations exceeding the value of the WHO (2022) guideline value of 80 µg/L recorded in the alluvial aquifer at P2 (113 µg/L) P3 (101 µg/L), B4 (985 µg/L) P6 (320 µg/L), P7 (474 µg/L) and P10 (289 µg/L) and in the CH aquifer at B8 (151 µg/L) and B18 (117 µg/L), threaten the suitability of groundwater for drinking-water supplies; the health consequences of excessive aqueous Mn have yet to be reported regionally.

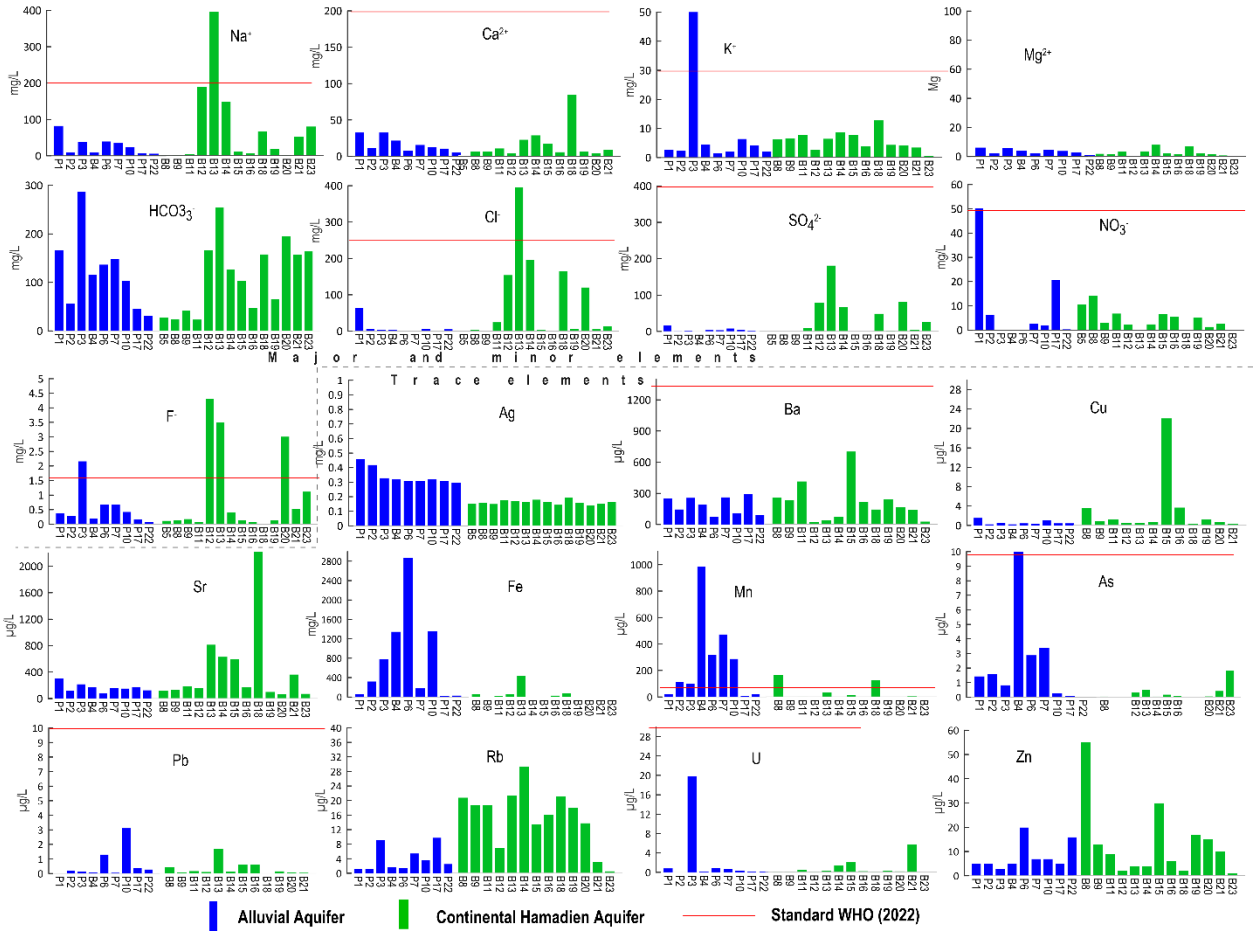

Fig. 9 Major ions and trace elements compositions of the alluvial and Continental Hamadien (CH) aquifer compared with WHO (2022) drinking-water quality guidelines.

Standard indicators of the suitability of groundwater for use in irrigation suggest, despite small differences among them, that groundwater in the alluvial is consistently viable whereas deeper groundwater in downstream locations of the CH aquifer may in places, be unsuitable. Based on the classification of the United States Soil Laboratory (USSL, 1954) (Fig. 10a), where EC is considered a salinity hazard and SAR is considered an alkalinity hazard (Bian et al. 2018; Zhao et al. 2021), 29% (5/17) of the samples of alluvial aquifer and 37% (6/16) of CH samples lie in the C1-S1 zone, with 47% (8/17) of the alluvial and 12% (2/16) of CH samples, respectively, fall within the C2-S1 zone. These first two zones are associated with low/medium salinity risk (C1/C2) and low sodium (S1) and thus considered suitable for irrigation on most soil types (clayey, silty and sandy soils). The remaining CH samples lie within the zones C3-S4 for two samples and C2-S4, C3-S2, and C3-S1, with one sample for each zone, and 1 and 3 samples for the last 2 classes

for the alluvial aquifer. The C2-S4 zone (medium salinity - high sodium hazard) suggests water that is only usable for irrigation of very sodium-tolerant plants. Zones C3-S1, C3-S2, and C3-S4 represent high salinity (C3) with, respectively, low sodium risk (S1), medium sodium risk (S2), and very high sodium risk (S4). According to Zhao et al. (2021), waters in zones C3-S1 and C3-S2 may be used on coarse-textured, well-drained soils. C3-S4 waters are deemed inadequate for irrigation as their use will cause damage to soils and plants. On the basis of the SAR indicator, the quality of the water in the shallow alluvial aquifer is more consistently suitable than the underlying groundwater in the CH aquifer. Further, based on Wilcox's (1955) classification (Fig. 10b), 77% (13/17) of samples from the shallow alluvial aquifer and 50% (8/16) of CH samples are considered to be good to excellent water for irrigation. 23% (4/17) and 6% (1/16) samples respectively for alluvial and CH aquifer are good to permissible. The remaining samples of CH fall into the classes of permissible to doubtful (3/16, 18%) and doubtful to unsuitable (4/16, 25%). Based on Richards's (1954) classification, for primary and secondary data (Table 5 and Table S2), 95% (16/17) samples of alluvial aquifer and 82% (13/16) of CH samples had RSC values < 2.5 meq/L, indicating the general suitability of sampled groundwater for irrigation. Nevertheless, 1/17 (5%) and 3/16 (18%) of the samples respectively from the alluvial and CH aquifer had an RSC > 2.5 meq/L. RSC values beyond +2.5 indicate a greater likelihood of Na^{+1} absorption by soil, restricting water and air movement through the soil. This, in turn, decreases soil permeability rendering it unsuitable for crop growth (Bian et al. 2018).

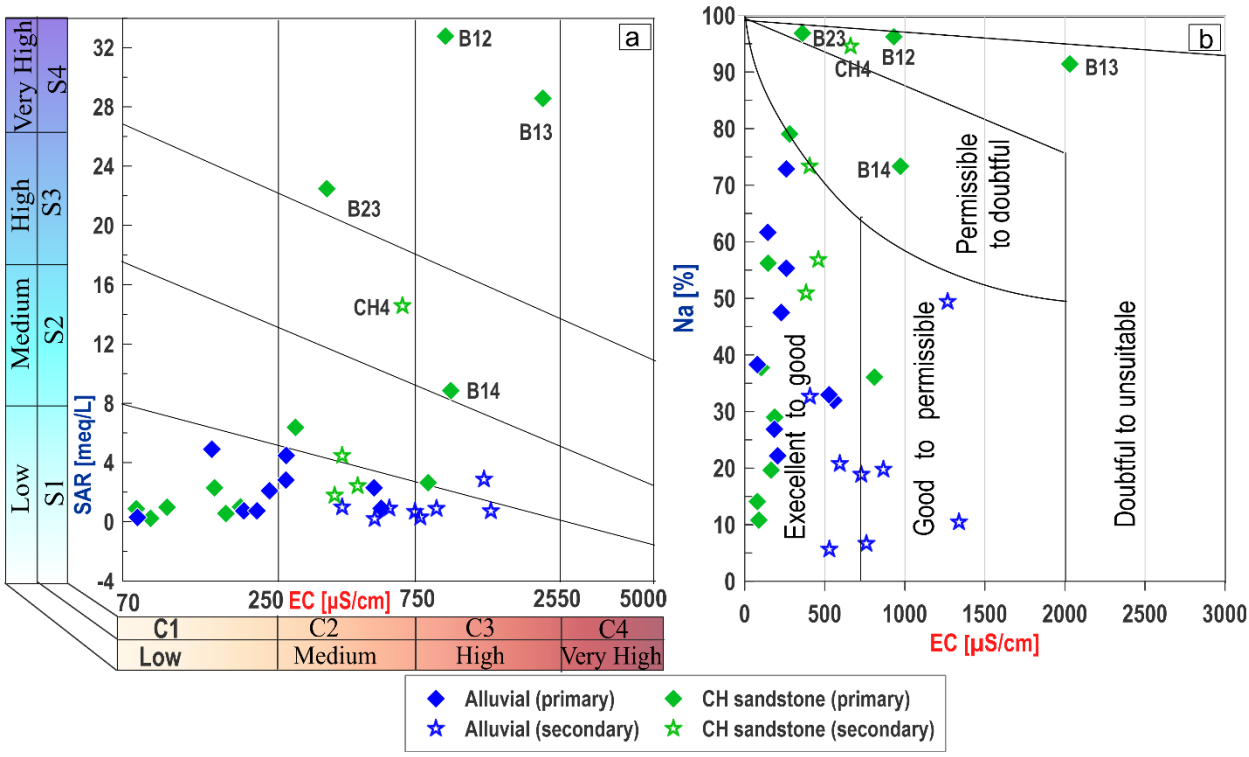

Fig. 10 Suitability of irrigation water for the alluvial and Continental Hamadien (CH) aquifers: **a** USSL Diagram, **b** Wilcox Diagram.

The results of this study have implications for the provision of drinking water and irrigation in the RBMG and similar environments in the Sahel. Groundwater in the alluvial aquifer is generally of an acceptable quality for drinking water and irrigation. Our results suggest that groundwater in the underlying CH aquifer in the upstream part of the basin, from depths of up to 100 m is also suitable for drinking and irrigation. In downstream locations of the RGMB at depths below 60 m, excessive locally fluoride concentrations in groundwater from some boreholes in the CH aquifer could present a potential risk to human health and be unsuitable for irrigation because of the high concentrations of sodium, chloride, sulfate, and fluoride. Better recognition of the spatial distribution of fluoride with depth and identification of the biogeochemical conditions and lithology favoring fluoride release will require a wider and depth-specific survey of groundwater quality. Our results constitute, however, a first step towards minimizing the risk to human health posed by high fluoride concentrations and constraints on the use of groundwater linked to domestic and agricultural water consumption. This study also contributes to understanding the mechanisms controlling groundwater mineralization and solute mobilization, including fluoride in the study

area. Fig. 11 provides a first conceptual model of the controls on, and risks to, groundwater quality in the RGMB.

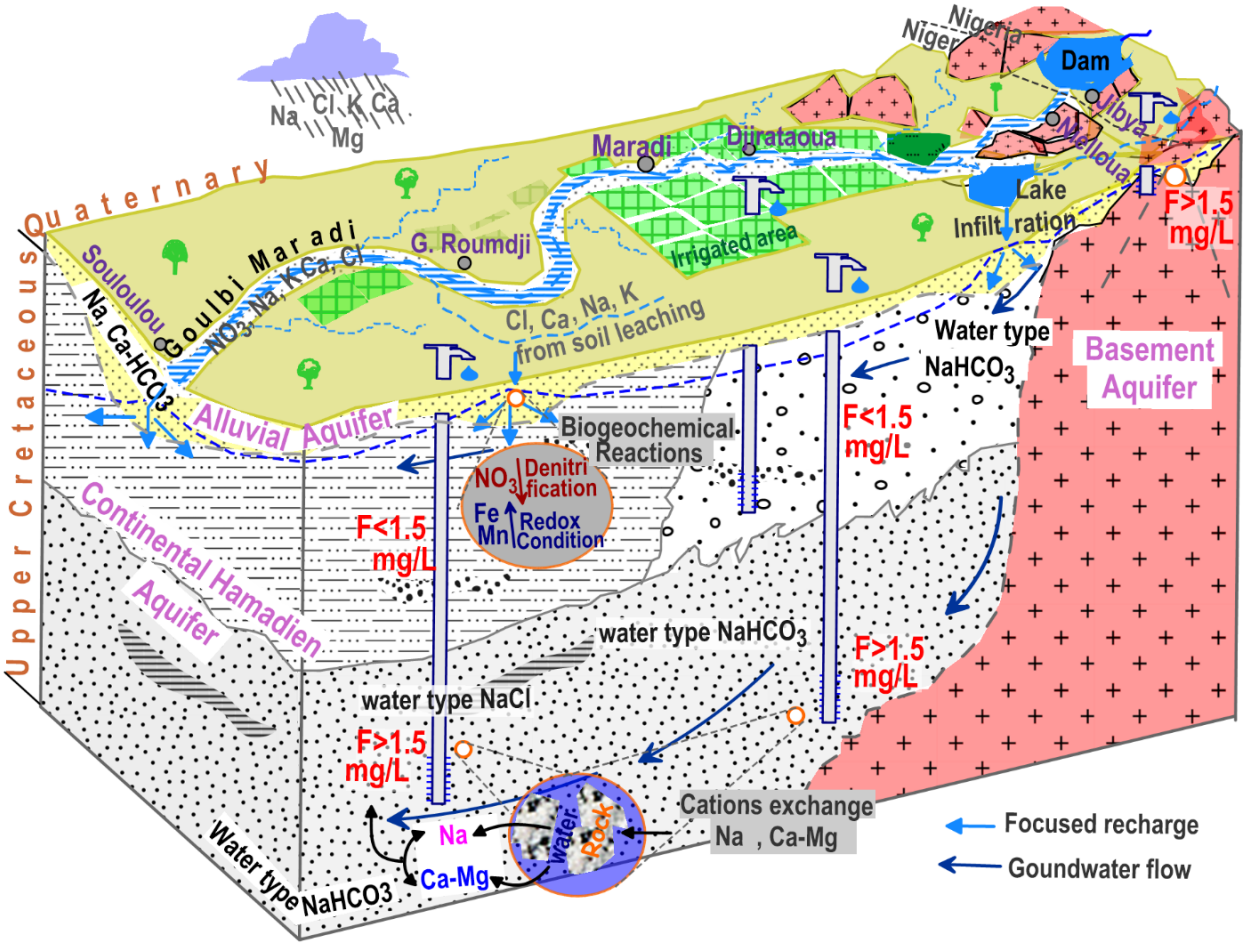

Fig. 11 Conceptual model of the geological, hydrological, and geochemical process controlling groundwater mineralization in the River Goulbi de Maradi Basin (RGMB).

Conclusion

New field observations from the transboundary River Goulbi Maradi Basin (RGMB) in southeastern Niger yield insight into the origin and quality of groundwater from a shallow alluvial aquifer and underlying regional sandstone aquifer, the Continental Hamadien (CH). Sampled groundwater is mainly of Na-HCO_3 and Ca-HCO_3 types in the alluvial aquifer and includes both Na-HCO_3 and Na-Cl types in the CH aquifer. Graphical and bivariate plots indicate the hydrochemistry of sampled groundwater is governed by rock-water interactions that include cation exchange. Solutes also derive from soil leaching from focused recharge events during the monsoon

period (June to early October). Based on primary datasets compiled here, groundwater sampled from 9 locations in the shallow alluvial aquifer mostly meets WHO (2022) drinking-water guidelines with 1 site presenting a fluoride concentration (2.2 mg/L) exceeding the threshold value of 1.5 mg/L; shallow groundwater is deemed suitable for use for irrigation according to a range of widely used indicators (i.e. SAR, %Na, RSC). Groundwater sampled from 12 locations in the CH aquifer included 2 co-located downstream sites where fluoride concentrations exceed drinking-water guidelines; and 3 locations with excessive solute concentrations that are unsuitable for use in irrigation. Potential sources of fluoride identified in the RGMB include the release of fluoride of geogenic origin through cation exchange, especially at depth in the CH aquifer, and localized 0use of fertilizers containing fluorapatite. Concentrations of manganese exceeded drinking-water guidelines in alluvial CH aquifers; the health consequences of this consumption have yet to be reported or resolved.

Acknowledgments The authors wish to acknowledge support from the *GroFutures* (Groundwater Futures in Sub-Saharan Africa - www.grofutures.org) research project funded by the NERC-ESRC-DFID (UK) UPGro program (refs. NE/M008576/1, NE/M008932/1). RGT acknowledges support of a Fellowship (ref. FL001275) from CIFAR (Canadian Institute for Advanced Research) under the Earth-4D program. The authors also acknowledge the participation of the Direction of Hydraulics and Sanitation of Maradi (Ministry of Hydraulics and Sanitation), especially Ms. Issoufa Ibrahim namely *Dingal*, for his assistance in field data collection.

Declarations

Conflict of interest The authors declare that they have no conflict of interest.

References

Abdou Babaye MS, Orban P, Ousmane B, Favreau G, Brouyère S & Dassargues A (2019) Characterization of recharge mechanisms in a Precambrian basement aquifer in semi-arid south-west Niger. *Hydrogeology Journal*, *27*(2), 475–491. https://doi.org/10.1007/s10040-018-1799-x

Abdou Mahaman R, Nazoumou Y, Favreau G, Issoufou Ousmane B, Boucher M, Abdou Babaye MS, Lawson FMA, Vouillamoz J.-M, Guéro A, Legchenko A & Taylor RG (2023) Paleochannel groundwater discharge to the River Niger in the Iullemmeden Basin estimated by near- surface geophysics and piezometry. *Environmental Earth Sciences*, *82*(9), 202. https://doi.org/10.1007/s12665-023-10861-y

Adams EA, Sambu D & Smiley SL (2018) Urban water supply in Sub-Saharan Africa: historical and emerging policies and institutional arrangements. *Https://Doi.Org/10.1080/07900627.2017.1423282*, *35*(2), 240–263. https://doi.org/10.1080/07900627.2017.1423282

Ali S, Thakur SK, Sarkar A & Shekhar S (2016) Worldwide contamination of water by fluoride. *Environmental Chemistry Letters 2016 14:3*, *14*(3), 291–315. https://doi.org/10.1007/S10311-016-0563-5

Altchenko Y & Villholth KG (2015) Mapping irrigation potential from renewable groundwater in Africa-A quantitative hydrological approach. *Hydrology and Earth System Sciences*, *19*(2), 1055–1067. https://doi.org/10.5194/hess-19-1055-2015

Baraou Idi S (2018) Contribution to the petrographic, geochronological, and structural study of the Pan-African formations of South Maradi (South Niger): relationships with gold showings. *PhD., Univ. Abdou Moumouni, Niamey, Niger.*

Bian J, Nie S, Wang R, Wan H & Liu C (2018) Hydrochemical characteristics and quality assessment of groundwater for irrigation use in central and eastern Songnen Plain, Northeast China. *Environmental Monitoring and Assessment*, *190*(7), 1–16. https://doi.org/10.1007/S10661-018-6774-4/FIGURES/5

Boubacar Hassane A, Leduc C, Favreau G, Bekins B A & Margueron T (2015) Impacts of a large Sahelian city on groundwater hydrodynamics and quality : example of Niamey (Niger). https://doi.org/10.1007/s10040-015-1345-z

BRGM (1978. Etudes comparatives du projet du Goulbi de Maradi : Evaluation et gestion des ressources en eaux souterraines du système des alluvions. *Rapport BRGM 78 AGE 017*.

Carter RC & Parker A (2009) Climate change, population trends and groundwater in Africa. *Hydrological Sciences Journal*, *54*(4), 676–689. https://doi.org/10.1623/hysj.54.4.676

Cobbing J (2020) Groundwater and the discourse of shortage in Sub-Saharan Africa. *Hydrogeology Journal*, *28*(4), 1143–1154. https://doi.org/10.1007/S10040-020-02147-5/FIGURES/1

Cobbing J & Hiller B (2019) Waking a sleeping giant: Realizing the potential of groundwater in Sub-Saharan Africa. *World Development*, *122*, 597–613. https://doi.org/10.1016/J.WORLDDEV.2019.06.024

Cuthbert MO, Taylor RG, Favreau G, Todd MC, Shamsudduha M, Villholth KG, MacDonald A M, Scanlon BR, Kotchoni DOV, Vouillamoz J, Lawson FMA, Adjomayi PA, Kashaigili J, Seddon D, Sorensen JPR, Ebrahim GY, Owor M, Nyenje PM, Nazoumou Y, … Kukuric N (2019) Observed controls on resilience of groundwater to climate variability in sub-Saharan Africa. *Nature*, *572*(7768), 230–234. https://doi.org/10.1038/s41586-019-1441-7

Davraz A & Özdemir A (2014) Groundwater quality assessment and its suitability in Çeltikçi plain (Burdur/Turkey). *Environmental Earth Sciences 2014 72:4*, *72*(4), 1167–1190. https://doi.org/10.1007/S12665-013-3036-1

Descroix L, Genthon P, Amogu O, Rajot J-L, Sighomnou D & Vauclin M (2012) Change in Sahelian Rivers hydrograph: The case of recent red floods of the Niger River in the Niamey region. *Global and Planetary Change*, *98–99*, 18–30. https://doi.org/10.1016/j.gloplacha.2012.07.009

Descroix L, Mahé G, Lebel T, Favreau G, Galle S, Gautier E, Olivry J-C, Albergel J, Amogu O, Cappelaere B, Dessouassi R, Diedhiou A, Le Breton E, Mamadou I & Sighomnou D (2009) Spatio-temporal variability of hydrological regimes around the boundaries between Sahelian

and Sudanian areas of West Africa: A synthesis. *Journal of Hydrology*, *375*(1–2), 90–102. https://doi.org/10.1016/j.jhydrol.2008.12.012

Dibal HU, Schoeneich K, Garba I, Lar UA & Bala EA (2012) Overview of fluoride distribution in major aquifer units of northern Nigeria. *Health*, *2012*(12), 1287–1294. https://doi.org/10.4236/HEALTH.2012.412189

Dikouma M (1990) Fluctuation du niveau marin au Maestrichtien et au Paléocène dans le bassin Intracratonique des Iullemmeden (Ader-Doutchi, Niger). *Thèse Doctorat, Univ. Dijon-Niamey,* 273p.

Durand A, Icole M, Bieda S (1981) Sédiments et climats quaternaires du Sahel central : exemple de la vallée de Maradi (Niger méridional). *UNIV., SERVICE GEOL./NIAMEY/NER, VOL. 12*; *N*(January 1981).

Eaton FM (1950) Significance of carbonates in irrigation waters. *Soil Science*, *69*, 123–134.

Edmunds WM & Smedley PL (2013) Fluoride in natural waters. In *Essentials of Medical Geology: Revised Edition* (pp. 311–336). Springer Netherlands. https://doi.org/10.1007/978-94-007-4375-5_13

Elagib NA, Zayed IS, Al Saad SAG, Mahmood MI, Basheer M & Fink AH (2021) Debilitating floods in the Sahel are becoming frequent. *Journal of Hydrology*, *599*, 126362. https://doi.org/10.1016/J.JHYDROL.2021.126362

Elbaz-Poulichet F, Favreau G, Leduc C & Seidel JL (2002) Major ion chemistry of groundwaters in the Continental Terminal water table of southwestern Niger (Africa). *Applied Geochemistry*, *17*(10), 1343–1349. https://doi.org/10.1016/S0883-2927(02)00024-0

Farid I, Trabelsi R, Zouari K, Abid K & Ayachi M (2013) Hydrogeochemical processes affecting groundwater in an irrigated land in Central Tunisia. *Environmental Earth Sciences*, *68*(5), 1215–1231. https://doi.org/10.1007/s12665-012-1788-7

Favreau G, Cappelaere B, Massuel S, Leblanc M, Boucher M, Boulain N & Leduc C (2009) Land clearing, climate variability, and water resources increase in semiarid southwest Niger: A review. *Water Resources Research*, *45*(7), 1–18. https://doi.org/10.1029/2007WR006785

Favreau G, Nazoumou Y, Leblanc M, Guéro A & Goni IB (2012) Groundwater resources increase in the Iullemmeden Basin, West Africa. *In Climate Change Effects on Groundwater Resources: A Global Synthesis of Findings and Recommendations (Pp. 113-128). CRC Press.*

FIDH (2002) Droit à l'eau potable au Niger Enfants de Tibiri : quand l'eau se transforme en poison Privatisation de la distribution de l'eau : un processus à surveiller. *Rapport Mission Internationale d'Enquête*, p.60

Fisher RS & Mullican III WF (1997) Hydrochemical Evolution of Sodium-Sulfate and Sodium-Chloride Groundwater Beneath the Northern Chihuahuan Desert, Trans-Pecos, Texas, USA. *Hydrogeology Journal*, *5*(2), 4–16. https://doi.org/10.1007/s100400050102

Foster S, Pulido-Bosch A, Vallejos Á, Molina L, Llop A & MacDonald AM (2018) Impact of irrigated agriculture on groundwater-recharge salinity: a major sustainability concern in semi-arid regions. *Hydrogeology Journal*, *26*(8), 2781–2791. https://doi.org/10.1007/S10040-018-1830-2/FIGURES/7

Gaye CB & Tindimugaya C (2019) Review: Challenges and opportunities for sustainable groundwater management in Africa. *Hydrogeology Journal*, *27*(3), 1099–1110. https://doi.org/10.1007/S10040-018-1892-1/FIGURES/1

Gleeson T, Wang-Erlandsson L, Porkka M, Zipper SC, Jaramillo F, Gerten D, Fetzer I, Cornell SE, Piemontese L, Gordon LJ, Rockström J, Oki T, Sivapalan M, Wada Y, Brauman KA, Flörke M, Bierkens MFP, Lehner B, Keys P, … Famiglietti JS (2020) Illuminating water cycle modifications and Earth system resilience in the Anthropocene. *Water Resources Research*, *56*(4), e2019WR024957. https://doi.org/10.1029/2019WR024957

Goni IB (2006) Tracing stable isotope values from meteoric water to groundwater in the southwestern part of the Chad basin. *Hydrogeology Journal*, *14*(5), 742–752. https://doi.org/10.1007/S10040-005-0469-Y/FIGURES/5

Goni IB, Taylor RG, Favreau G, Shamsudduha M, Nazoumou Y & Ngounou Ngatcha B. (2021). Groundwater recharge from heavy rainfall in the southwestern Lake Chad Basin: evidence from isotopic observations. *Hydrological Sciences Journal*, *66*(8), 1359–1371. https://doi.org/10.1080/02626667.2021.1937630/SUPPL_FILE/THSJ_A_1937630_SM5432

.DOCX

Greigert J (1966) Description des formations crétacées et tertiaires du bassin des Iullemmeden. *Rapport BRGM,Orléans, France*. 236.

Haji M, Wang D, Li L, Qin D & Guo Y (2018) Geochemical Evolution of Fluoride and Implication for F− Enrichment in Groundwater: Example from the Bilate River Basin of Southern Main Ethiopian Rift. *Water*, *10*(12), 1799. https://doi.org/10.3390/w10121799

Hazell JRT, Cratchley CR & Jones CRC (1992) The hydrogeology of crystalline aquifers in northern Nigeria and geophysical techniques used in their exploration. *Geological Society Special Publication*, *66*, 155–182. https://doi.org/10.1144/GSL.SP.1992.066.01.08

Homoncik SC, MacDonald AM, Heal KV, Ó Dochartaigh BÉ & Ngwenya BT (2010) Manganese concentrations in Scottish groundwater. Science of The Total Environment, 408(12), 2467–2473. https://doi.org/10.1016/J.SCITOTENV.2010.02.017

Huang L, Sun Z, Zhou A, Bi J & Liu Y (2022) Source and enrichment mechanism of fluoride in groundwater of the Hotan Oasis within the Tarim Basin, Northwestern China. *Environmental Pollution*, *300*, 118962. https://doi.org/10.1016/j.envpol.2022.118962

Ibrahim M, Favreau G, Scanlon BR, Seidel JL, Le Coz M, Demarty J & Cappelaere B (2014). Long-term increase in diffuse groundwater recharge following expansion of rainfed cultivation in the Sahel, West Africa. *Hydrogeology Journal*, *22*(6), 1293–1305. https://doi.org/10.1007/s10040-014-1143-z

Ijumulana J, Ligate F, Bhattacharya P, Mtalo F & Zhang C (2020) Spatial analysis and GIS mapping of regional hotspots and potential health risk of fluoride concentrations in groundwater of northern Tanzania. *Science of The Total Environment*, *735*, 139584. https://doi.org/10.1016/J.SCITOTENV.2020.139584

INS (2012) Recensement Général de la Population et de l'Habitat 2012. NER-INS-RGPH-2012-V1.0. https://doi.org/http://anado.ins.ne/index.php

INS (2018) Annuaire statistique régional de Maradi 2013-2017. *Edition 2018.* 1–260.

Issa Lélé M & Lamb PJ (2010) Variability of the Intertropical Front (ITF) and Rainfall over the West African Sudan–Sahel Zone. *Journal of Climate*, *23*(14), 3984–4004. https://doi.org/10.1175/2010JCLI3277.1

Issoufou Ousmane B, Nazoumou Y, Favreau G, Abdou Babaye MS, Abdou Mahaman R, Boucher B, Lawson FMA, Taylor RG, Legchenko A (2021) Caractérisation géophysique des aquifères dans la vallée transfrontalière du Goulbi de Maradi (Niger/Nigeria). 12e Colloque GEOFCAN, 05–08. Retrieved from. https://hal.inrae.fr/hal-03145437

Issoufou Ousmane B, Nazoumou Y, Favreau G, Abdou Babaye MS, Abdou Mahaman R, Boucher M, Issoufa I, Lawson FMA, Vouillamoz J-M, Legchenko A & Graham Taylor R (2022) Changes in aquifer properties along a seasonal river channel of the Niger Basin: Identifying groundwater recharge pathways in a dryland environment. *Journal of African Earth Sciences*, 104742. https://doi.org/10.1016/j.jafrearsci.2022.104742

Karroum M, Elgettafi M, Elmandour A, Wilske C, Himi, M & Casas A (2017) Geochemical processes controlling groundwater quality under semi arid environment: A case study in central Morocco. *Science of The Total Environment*, *609*, 1140–1151. https://doi.org/10.1016/J.SCITOTENV.2017.07.199

Korom SF (1992) Natural denitrification in the saturated zone: A review. *Water Resources Research*, *28*(6), 1657–1668. https://doi.org/10.1029/92WR00252

Kundu MC & Mandal B (2009) Assessment of potential hazards of fluoride contamination in drinking groundwater of an intensively cultivated district in West Bengal, India. *Environmental Monitoring and Assessment*, *152*(1–4), 97–103. https://doi.org/10.1007/S10661-008-0299-1/METRICS

Kut KMK, Sarswat A, Srivastava A, Pittman CU & Mohan D (2016) A review of fluoride in african groundwater and local remediation methods. *Groundwater for Sustainable Development*, *2–3*, 190–212. https://doi.org/10.1016/J.GSD.2016.09.001

Laatar A, Mrabet D & Zakraoui L (2003) La fluorose en Afrique subsaharienne. *Revue Du Rhumatisme*, *70*(2), 178–182. https://doi.org/10.1016/S1169-8330(02)00032-7

Lapworth DJ, Baran N, Stuart ME & Ward RS (2012) Emerging organic contaminants in groundwater: A review of sources, fate and occurrence. *Environmental Pollution*, *163*, 287–303. https://doi.org/10.1016/J.ENVPOL.2011.12.034

Lapworth DJ, Boving TB, Kreamer DK, Kebede S & Smedley PL (2022) Groundwater quality: Global threats, opportunities and realising the potential of groundwater. *Science of The Total Environment*, *811*, 152471. https://doi.org/10.1016/j.scitotenv.2021.152471

Lapworth DJ, Krishan G, MacDonald AM & Rao MS (2017) Groundwater quality in the alluvial aquifer system of northwest India: New evidence of the extent of anthropogenic and geogenic contamination. *Science of The Total Environment*, *599–600*, 1433–1444. https://doi.org/10.1016/J.SCITOTENV.2017.04.223

Lapworth DJ, MacDonald AM, Kebede S, Owor M, Chavula G, Fallas H, Wilson P, Ward JST, Lark M, Okullo J, Mwathunga E, Banda S, Gwengweya G, Nedaw D, Jumbo S, Banks E, Cook P & Casey V (2020) Drinking water quality from rural handpump-boreholes in Africa. Environmental Research Letters, 15(6), 064020. https://doi.org/10.1088/1748-9326/AB8031

Lebel T & Ali A (2009) Recent trends in the Central and Western Sahel rainfall regime (1990–2007). *Journal of Hydrology*, *375*(1–2), 52–64. https://doi.org/10.1016/j.jhydrol.2008.11.030

Leblanc MJ, Favreau G, Massuel S, Tweed SO, Loireau M & Cappelaere B (2008) Land clearance and hydrological change in the Sahel: SW Niger. *Global and Planetary Change*, *61*(3–4), 135–150. https://doi.org/10.1016/J.GLOPLACHA.2007.08.011

Li P, He X, Li Y & Xiang G (2019) Occurrence and Health Implication of Fluoride in Groundwater of Loess Aquifer in the Chinese Loess Plateau: A Case Study of Tongchuan, Northwest China. *Exposure and Health*, *11*(2), 95–107. https://doi.org/10.1007/s12403-018-0278-x

Li P, Wu J & Qian H (2016) Hydrochemical appraisal of groundwater quality for drinking and irrigation purposes and the major influencing factors: a case study in and around Hua County, China. *Arabian Journal of Geosciences*, *9*(1), 15. https://doi.org/10.1007/s12517-015-2059-1

Li P, Zhang Y, Yang N, Jing L & Yu P (2016) Major ion chemistry and quality assessment of groundwater in and around a mountainous tourist town of China. *Exposure and Health*, *8*(2),

239–252. https://doi.org/10.1007/s12403-016-0198-6

Liu J, Wang M, Gao Z, Chen Q, Wu G & Li F (2020) Hydrochemical characteristics and water quality assessment of groundwater in the Yishu River basin. *Acta Geophysica*, *68*(3), 877–889. https://doi.org/10.1007/s11600-020-00440-1

MacDonald AM, Bonsor HC, Dochartaigh BÉÓ & Taylor RG (2012) Quantitative maps of groundwater resources in Africa. *Environmental Research Letters*, *7*(2), 024009. https://doi.org/10.1088/1748-9326/7/2/024009

Mahe G, Lienou G, Descroix L, Bamba F, Paturel JE, Laraque A, Meddi M, Habaieb H, Adeaga O, Dieulin C, Chahnez Kotti F & Khomsi K (2013) The rivers of Africa: witness of climate change and human impact on the environment. *Hydrological Processes*, *27* (15), 2105–2114. https://doi.org/10.1002/HYP.9813

Mahe G, Paturel J-E, Servat E, Conway D & Dezetter A (2005) The impact of land use change on soil water holding capacity and river flow modelling in the Nakambe River, Burkina-Faso. *Journal of Hydrology*, *300*(1–4), 33–43. https://doi.org/10.1016/j.jhydrol.2004.04.028

Mar SS & Okazaki M (2012) Investigation of Cd contents in several phosphate rocks used for the production of fertilizer. *Microchemical Journal*, *104*, 17–21. https://doi.org/10.1016/J.MICROC.2012.03.020

MHA (2016) Pragramme sectoriel eau hygiene et assainissement. Rapport du Ministère de l'Hydraulique et de l'assainissement.

MHA (2020) Rapport annuel d'activités du Ministère de l'Hydraulique et de l'assainissement.

Mignon R (1970) Étude géologique et prospection du Damagaram Mounio et du Sud Maradi.

Nazoumou Y, Favreau G, Adamou MM & Maïnassara I (2016) La petite irrigation par les eaux souterraines, une solution durable contre la pauvreté et les crises alimentaires au Niger ? *Cahiers Agricultures*, *25*(1), 15003. https://doi.org/10.1051/cagri/2016005

Nordstrom DK & Smedley PL (2022) Fluoride in groundwater. *Fluoride*.

Olaka LA, Wilke FDH, Olago DO, Odada EO, Mulch A & Musolff A (2016) Groundwater fluoride

enrichment in an active rift setting: Central Kenya Rift case study. *Science of The Total Environment*, *545–546*, 641–653. https://doi.org/10.1016/j.scitotenv.2015.11.161

Onipe T, Edokpayi JN & Odiyo JO (2020) A review on the potential sources and health implications of fluoride in groundwater of Sub-Saharan Africa. *Https://Doi.Org/10.1080/10934529.2020.1770516*, *55*(9), 1078–1093. https://doi.org/10.1080/10934529.2020.1770516

OSS (2008) Système aquifère d'Iullemeden (Mali, Niger, Nigeria): gestion concertée des ressources en eau partagées d'un aquifère transfrontalier sahélien. *OSS, Rapport technique*.

Parkhurst DL & Appelo CAJ (2013) Description of input and examples for PHREEQC version 3: a computer program for speciation, batch-reaction, one-dimensional transport, and inverse geochemical calculations. *Techniques and Methods*. https://doi.org/10.3133/TM6A43

Piper AM (1944) A graphic procedure in the geochemical interpretation of water-analyses. *Eos, Transactions American Geophysical Union*, *25*(6), 914–928. https://doi.org/10.1029/TR025I006P00914

Podgorski J & Berg M (2022) Global analysis and prediction of fluoride in groundwater. *Nature Communications 2022 13:1*, *13*(1), 1–9. https://doi.org/10.1038/s41467-022-31940-x

Rafique T, Naseem S, Ozsvath D, Hussain R, Bhanger MI & Usmani TH (2015) Geochemical controls of high fluoride groundwater in Umarkot Sub-District, Thar Desert, Pakistan. *Science of The Total Environment*, *530–531*, 271–278. https://doi.org/10.1016/j.scitotenv.2015.05.038

Rajmohan N, Masoud MHZ & Niyazi BAM (2021) Impact of evaporation on groundwater salinity in the arid coastal aquifer, Western Saudi Arabia. *CATENA*, *196*, 104864. https://doi.org/10.1016/J.CATENA.2020.104864

Richards LA (1954) Diagnosis and Improvement of Saline and Alkali Soils. In *Soil Science* (Vol. 78).

Rivett MO, Buss SR, Morgan P, Smith JWN & Bemment CD (2008) Nitrate attenuation in groundwater: A review of biogeochemical controlling processes. *Water Research*, *42*(16),

4215–4232. https://doi.org/10.1016/J.WATRES.2008.07.020

Schoeller H (1965) Qualitative evaluation of groundwa-ter resource. In *Methods and techniques of groundwater investigations and development. UNESCO Water Resources Series* (pp. 44–52).

Su H, Wang J & Liu J (2019) Geochemical factors controlling the occurrence of high-fluoride groundwater in the western region of the Ordos basin, northwestern China. *Environmental Pollution*, *252*, 1154–1162. https://doi.org/10.1016/j.envpol.2019.06.046

Subba Rao N, Marghade D, Dinakar A, Chandana I, Sunitha B, Ravindra B & Balaji T (2017) Geochemical characteristics and controlling factors of chemical composition of groundwater in a part of Guntur district, Andhra Pradesh, India. *Environmental Earth Sciences*, *76*(21), 747. https://doi.org/10.1007/s12665-017-7093-8

Taylor RG, Aureli A, Allen DA, Banks D, Villholth KG and Stigter T (2022) Groundwater, Aquifers and Climate Change (Chapter 7). In The United Nations World Water Development Report 2022: Groundwater: Making the invisible visible. UNESCO (Paris), pp. 101-114.

Taylor RG, Scanlon B, Döll P, Rodell M, Van Beek R, Wada Y, Longuevergne L, Leblanc M, Famiglietti JS, Edmunds M, Konikow L, Green TR, Chen J, Taniguchi M, Bierkens MFPP, MacDonald A, Fan Y, Maxwell RM, Yechieli Y, … Treidel H (2013) Ground water and climate change. *Nature Climate Change*, *3*(4), 322–329. https://doi.org/10.1038/nclimate1744

Travi Y (1988) Hydrogeochemistry and Hydrogeology of the Aquifers Fluorinated Basin of Senegal. Origin and Transport Conditions of Fluoride in Groundwater. University of Paris-Sud.

Tschakert P, Sagoe R, Ofori-Darko G & Codjoe SN (2010) Floods in the Sahel: an analysis of anomalies, memory, and anticipatory learning. *Climatic Change 2009 103:3*, *103*(3), 471–502. https://doi.org/10.1007/S10584-009-9776-Y

Tukur AN & Akobundu A (2014) Fluoride Contamination of Shallow Groundwater in Parts of Zango Local Government Area of Katsina State, Northwest Nigeria. *Journal of Geosciences and Geomatics*, *2*(5), 178–185. https://doi.org/10.12691/JGG-2-5-1

Tweed S, Leblanc M, Cartwright I, Favreau G & Leduc C (2011) Arid zone groundwater recharge and salinisation processes; an example from the Lake Eyre Basin, Australia. *Journal of Hydrology*, *408*(3–4), 257–275. https://doi.org/10.1016/J.JHYDROL.2011.08.008

UN (2019) *Revision of World Population Prospects*. https://population.un.org/wpp/

USSL (1954) Diagnosis and Improvement of Saline and Alkaline Soils. *Soil Science Society of America Journal*, *18*(3), 348. https://doi.org/10.2136/sssaj1954.03615995001800030032x

Wang Y, Li J, Ma T, Xie X, Deng Y & Gan Y (2020) Genesis of geogenic contaminated groundwater: As, F and I. *Https://Doi.Org/10.1080/10643389.2020.1807452*, *51*(24), 2895–2933. https://doi.org/10.1080/10643389.2020.1807452

WHO (2019) *Drinking-water*.

WHO (2022) *Guidelines for drinking-water quality: fourth edition incorporating the first and second addenda* (Vol. 33, Issue 33).

Wilcox LV (1948) The Quality of Water for Irrigation Use, *US Department of Agriculture, Technical Bulletin No. 962, Washington, D.C.,*.

Wilcox LV (1955) *Classification and use of irrigation waters*. 969.

Xu P, Bian J, Li Y, Wu J, Sun X & Wang Y (2022) Characteristics of fluoride migration and enrichment in groundwater under the influence of natural background and anthropogenic activities. *Environmental Pollution*, *314*, 120208. https://doi.org/10.1016/J.ENVPOL.2022.120208

Xu Y, Seward P, Gaye C, Lin L & Olago DO (2019) Preface: Groundwater in Sub-Saharan Africa. *Hydrogeology Journal*, *27*(3), 815–822. https://doi.org/10.1007/S10040-019-01977-2/FIGURES/1

Zaman M, Shahid SA & Heng L (2018) Irrigation Water Quality. *Guideline for Salinity Assessment, Mitigation and Adaptation Using Nuclear and Related Techniques*, 113–131. https://doi.org/10.1007/978-3-319-96190-3_5

Zhao X, Guo H, Wang Y, Wang G, Wang H, Zang X & Zhu J (2021) Groundwater hydrogeochemical characteristics and quality suitability assessment for irrigation and drinking purposes in an agricultural region of the North China plain. *Environmental Earth Sciences*, *80*(4), 1–22. https://doi.org/10.1007/S12665-021-09432-W/FIGURES/5